Research Square

Preprints are preliminary reports that have not undergone peer review.
They should not be considered conclusive, used to inform clinical practice,
or referenced by the media as validated information.

Energy-intensive adaptation partially offsets climate-driven labour productivity losses but at rising welfare costs

Gabriele Campoleoni Mansi

gabriele.mansi@cmcc.it

CMCC / Ca Foscari University https://orcid.org/0000-0003-4392-6295

Francesco Colelli

CMCC

Laurent Drouet

RFF-CMCC European Institute on Economics and the Environment (EIEE) https://orcid.org/0000-0002-4087-7662

Article

Keywords:

Posted Date: July 24th, 2026

DOI: https://doi.org/10.21203/rs.3.rs-10359395/v1

License: This work is licensed under a Creative Commons Attribution 4.0 International License.
Read Full License

Additional Declarations: There is **NO** Competing Interest.

Energy-intensive adaptation partially offsets climate-driven labour productivity losses but at rising welfare costs

Campoleoni Mansi G. A.[1,2,3], Colelli F.[1,2], Drouet L.[1,2,4]

[1] CMCC Foundation - Euro-Mediterranean Center on Climate Change, Via Marco Biagi 5, Lecce, 73100, Italy
[2] RFF-CMCC European Institute on Economics and the Environment, Via Bergognone 34, Milan, 20144, Italy
[3] CaFoscari University, Dorsoduro 3246, Venice, 30123, Italy
[4] CENSE - Center for Environmental and Sustainability Research & CHANGE - Global Change and Sustainability Institute, NOVA School of Science and Technology, NOVA University Lisbon, Campus de Caparica, 2829-516 Caparica, Portugal

14-7-2026

Abstract

Climate change poses significant risks to the global labour force, as rising temperatures undermine both work capacity and health. This study investigates the feedbacks between temperature extremes and labour productivity and the role of increased energy consumption as a form of autonomous adaptation over the long run. We find that climate-induced labour impacts generate considerable losses and rising adaptation costs even under a moderate (SSP2) warming scenario, with global GDP falling by 2.9% per year by 2100. Results are robust in showing how the negative effect on labour significantly penalises highly exposed economies in the Global South, where exposure to rising temperature is highest and adaptive capacity is most limited, with annual GDP losses of -5.9% by 2100. High-income regions of the Global North, facing milder thermal stress and lower vulnerability, gain about 1.8%. Because the heat penalty falls on outdoor labour, which has no cooling channel, outdoor-intensive economies (India, Sub-Saharan Africa) lose the most.

Energy-intensive adaptation partially reverses these losses by an amount that grows with energy use, offsetting 18-40% of Global South's loss and flattening the heat-productivity slope by about 29%, but remains bounded by each region's thermal balance and installed cooling stock. Critically, adaptation response exhibits diminishing returns on additional energy, possibly leading to maladaptation pathways: unconstrained adaptation proves not being cost-effective in most of the cold-relief North and hot but energy-rich Southern economies. Adaptation through energy-intensive cooling solutions is therefore best understood as a targeted instrument with a region-specific optimal level.

Main

Climate change represents a growing threat to global labour through the increasing frequency and intensity of temperature extremes. Rising temperatures affect economic activity through multiple channels, including reductions in labour productivity, increases in heat-related morbidity, and higher healthcare expenditures [1][2]. Increasing temperatures directly impact labour supply (working hours) by altering time allocation to work [3], especially in climate-exposed sectors such as agriculture and construction [4][5][6], as workers seek to avoid heat-induced issues such as exhaustion, stroke, or even death [7][8][9]. Additionally, heat stress reduces labour productivity during these work hours, with workers experiencing severe heat stress needing more frequent breaks for hydration and/or cooling [9][10], while elevated body temperatures and dehydration can also lead to increased mistakes and accidental injuries [11][12][13]. Unmitigated temperature shocks on the working population are projected to further

reduce economic activity and growth, particularly in low- and middle-income countries [14][15], exacerbating inequality and poverty [16].

At the same time, households and firms respond to thermal stress through adaptive behaviour, most notably by increasing energy consumption for cooling services, when faced by permanent slowly evolving climatic changes with respect to their own past climatic exposure [17][18][19]. This can be referred as a form of autonomous adaptation, which is the adjustments made by households and firms particularly through the more intensive use of adaptive appliances. Over longer periods, agents perceive repeated temperature regimes as climatic shifts, prompting more significant adjustments, such as households without air conditioning purchasing one, and can be classified as a planned adaptation response. In the residential sector, AC could grow from 27% to 41% by 2050, implying up to a doubling of residential cooling electricity consumption, with he share of households with at least one appliance of about 47% to 65% under high-end emission scenarios, switching from the current 1.8 billion individuals to about 3.8 billion [20][19]. While a growing literature investigates AC adoption as a heat adaptation strategy for domestic cooling estimates for non-residential cooling such as in industry, manufacture, or agriculture are scarcer, with very few empirical estimates on the projected energy use in economic sectors [21].

Moreover, increased energy use for adaptation will likely remain highly unequal within and across countries and income groups [20], with significant regressive impacts and distributional implications, especially in lower-income regions of the Global South [22], which are expected to experience the highest frequency of extreme heat days with the least adaptation capacity. This overlap defines an energy-poverty trap in adaptation: the same regions facing the most intense heat are those with the least access to the cooling energy that could offset it. Limited energy access risks may amplify, rather than attenuating, the underlying North-South disparity in climate impacts, so that distributional gaps in energy access reinforce the geography of climate-driven welfare losses.

We investigate the joint interaction between climate-induced labour productivity losses and energy-based adaptation, integrating these channels within a unified modelling framework built on the WITCH Integrated Assessment Model [26] to 2100. This allows for consistent treatment of feedback effects between energy demand in productive sectors, capital accumulation in cooling technologies, and economy outcomes, to assess long-term economic implications, new energy and emissions trends and costs and effectiveness of adaptation.

This paper contributes to the literature in three main ways. First, it provides an integrated assessment of heat-induced labour productivity losses across sectors with differing exposure to thermal stress, distinguishing high-exposure sectors such as agriculture and construction [4][5][6] from more sheltered, low-exposure sectors, within a single dynamic modelling framework, whereas existing studies have generally analysed sector-specific impacts in isolation [14][15]. Second, by explicitly modelling capital accumulation in cooling technologies alongside sectoral energy demand, the paper extends the adaptation literature beyond the residential sector intensive margin [21], offering, to our knowledge, among the first long-term projections of non-residential cooling needs and their role in offsetting productivity losses. Third, by embedding both channels within a unified economy-energy framework to 2100, the paper quantifies the net effect of climate-induced heat stress on aggregate GDP, and assesses the extent to which energy-based adaptation can mitigate these losses, providing new evidence on the economic benefits and costs of adaptation investment.

Impact of climate extremes on labour productivity

We evaluated the impact of climate change on the working force through temperature-induced labour productivity loss. The evolution of productivity depends on projected temperature extremes, namely changes in Cooling Degree Days above 18°C (CDD18) and Heating Degree Days below 18°C (HDD18), relative to historical level. Formally, the climate signal enters economy as a proportional, exposure-weighted shock relative to a baseline SSP2 [23][24] productivity path. In this Impact Scenario (IS), the cooling capital stock is held at its historic level, so the reported effects isolate the gross labour-productivity damage prior to any endogenous energy use for adaptation. Across

the seventeen WITCH regions, the labour-productivity channel resolves into a clear feedback mechanism that systematically penalises regions in the Global South, where exposure to rising temperature is highest and adaptive capacity is more limited, while comparatively benefits high-income regions in the Global North, which experience milder thermal stress and lower baseline vulnerability.

Under the SSP2 baseline, projected global warming increases temperature anomalies: it raises cooling-degree days ($\Delta\mathrm{CDD18} > 0$) and lowers heating-degree days ($\Delta\mathrm{HDD18} < 0$), so that productivity is pulled in opposite directions by an intensifying heat penalty and a diminishing cold penalty (the cold-related productivity loss). Global means in 2100 show a cross-country average increase in CDD18s of 26.4% (+387/y) and decrease in HDD18s of -20% (-260/y), with respect to 2020 level.

The Net Thermal Balance, defined as the the algebraic sum of the difference between historic and projected temperature extremes ($NTB = \Delta\mathrm{CDD18} + \Delta\mathrm{HDD18}$), summarises which force prevails and determines the sign of the productivity response in every region. Where cold relief dominates ($NTB < 0$) a productivity gain occurs relative to baseline, whereas regions in which added heat dominates ($NTB > 0$) record a loss (Table 2, Figure 1). Since cooling and heating degree-days carry essentially the same weight on the final impact, the net thermal balance therefore captures the climate signal with a single variable (Table 3, col. 1, 2). The cross-regional correlation between *NTB* and the change in total factor productivity ($\Delta\mathrm{TFP}$), indicates that the climate extremes accounts for both the sign and almost the entire magnitude of the labour-productivity shock in 2100. This translates in about one percent of change in labour productivity for every ± 109 net degree-days, depending on absolute positive or negative net thermal balance.

Under the SSP2 baseline, the 2100 global-mean climate signal shows an average warming of 127 net degree-days with respect to 2020, which implies an Impact Scenario's mean productivity drag of -1.11% in 2050 and -2.04% in 2070 and -3.56% 2100. However, the global average masks a wide dispersion driven by the sign of the net balance: cold, high-latitude economies are characterized by negative *NTB* and productivity gain, while hot, tropical economies sit far on the positive side and bear the highest losses. The aggregate is mild precisely because the two groups pull in opposite directions, determining a redistribution of the overall impacts, not just a level effect. While the net balance explains the sign and most of the magnitude, the residual variation is governed by the structure of the economy, namely the split between indoor (low-exposure) and outdoor (high-exposure) labour (Table 3, col. 3). Holding the thermal balance fixed, an economy with 10 points more indoor work loses about 0.39% less productivity, because the heat penalty falls on outdoor labour, which is more severely impacted and has no (historic) cooling-adaptation channel. In short, heat and cold weigh equally but, for a given *NTB*, how hard a region is hit depends on his indoor vs outdoor labour share.

Consequently outdoor-intensive economies may lose substantially more than their thermal balance alone would imply. Relative to the fitted *TFP/NTB* relationship, India, South Asia and Sub-Saharan Africa lie respectively 1.50, 0.94 and 0.83 percentage points below the line, whereas a more indoor-intensive region such as Middle East and North Africa (which includes Gulf countries) lies 1.94 points above it despite a very large cooling-degree-day anomaly (Figure 2, top and bottom righ).

The mechanism is structural: the heat penalty falls on outdoor labour, which also carries no cooling-adaptation channel, so economies with a smaller indoor share (averaging 63% in the Global South against 77% in the North) convert a given thermal balance into larger productivity losses. The portion of the damage that would survive any future scale-up of cooling capital is therefore concentrated in precisely these outdoor-exposed regions.

These forces map onto a North-South divergence that widens monotonically over the century. Averaged across regions, the Global North gains 0.81%, 1.22% and 1.65% of productivity in 2050, 2070 and 2100, while the Global South loses -1.89%, -3.17% and -5.03%, a productivity wedge of about 6.7 percentage points by 2100. The spread proves to be climate-driven rather than developmental, and largely homogeneous within the two groups, with only two exceptions: China, which lies on the gain side (0.26% in 2100) because the substantial cold relief in its northern latitudes nearly offsets its heat exposure; and Oceania, which incurs a loss (-1.98%) due to its positive

NTB. In both, geography rather than economic structure determines the outcome.

The output response inherits this structure and amplifies it. Because the productivity shock is permanent, it shifts the steady-state capital stock, so GDP moves by more than TFP: across the loss-making regions the ratio $\Delta\text{GDP}/\Delta\text{TFP}$ is close to 1.3. While the global average GDP loss deepens from -0.3% in 2050 to -1.08% in 2070 and -2.9% 2100, the Global South's mean output loss to -1.49%, -3.07% and -5.87% over the three horizons, against Northern gains of 0.88%, 1.37% and 1.8%, widening the cross-regional wedge to about 7.7 percentage points in 2100. The deepest end-of-century output losses fall on India (-11.65%) and Sub-Saharan Africa (-8.78%), while the largest gains accrue to Canada (5.18%); full regional detail is reported in Table 2.

These figures constitute the upper-bound of climate change impact, as they precede the energy-intensive response for adaptation, mainly through the air-conditioning channel.

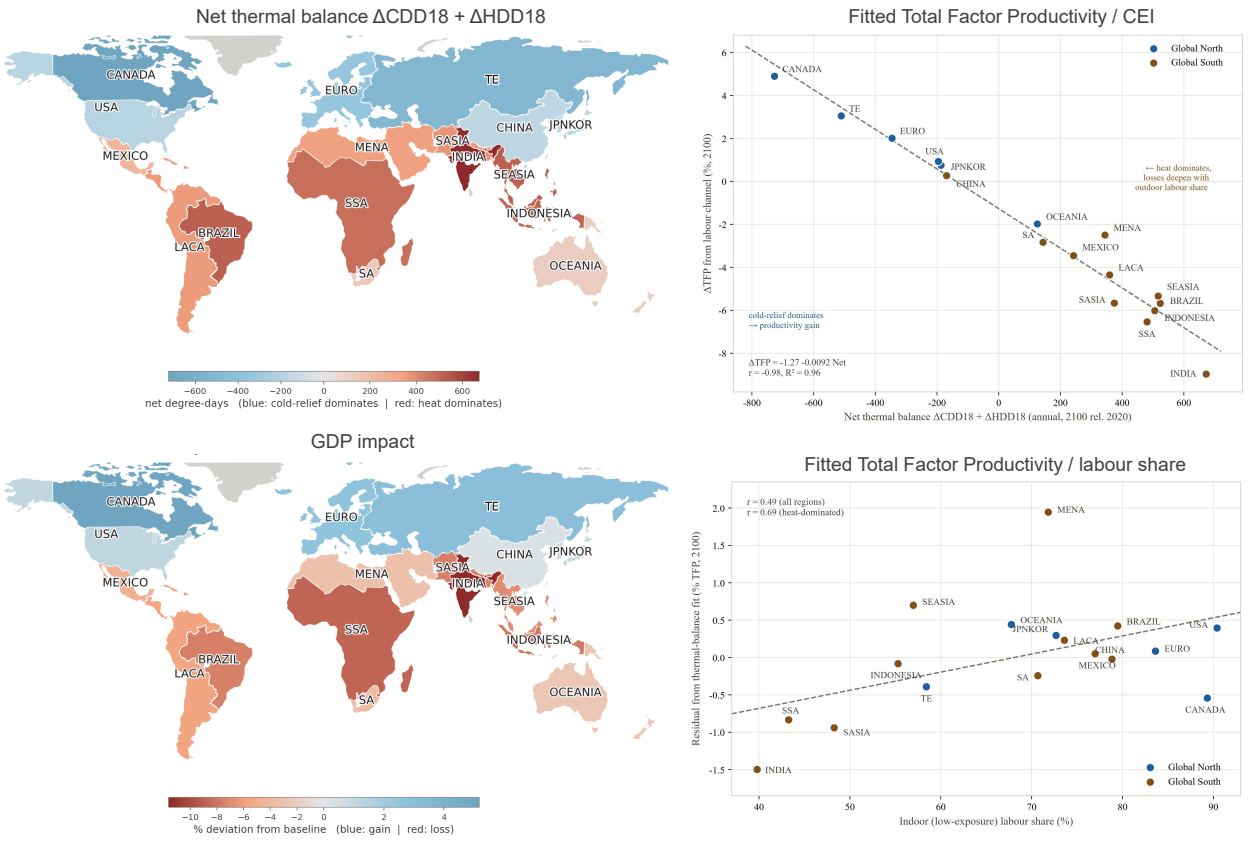


Figure 1 | Climate (temperature) anomaly projections and their welfare impact. The labour-productivity channel of warming follows the net thermal balance, whose sign sets the direction of the productivity response, while the structure of the economy, i.e. the shares between indoor and outdoor labour, governs its magnitude.

Top-left: End-of-century (2100) change in the net thermal balance ($\text{NTB} = \Delta\text{CDD18} + \Delta\text{HDD18}$), relative to 2020 under the SSP2 baseline, by WITCH region. Blue marks regions where the easing of cold exposure dominates ($\text{NTB} < 0$); red marks regions where intensifying heat dominates ($\text{NTB} > 0$). **Bottom-left:** Corresponding GDP impact in 2100, expressed as the percentage deviation of the labour-impact scenario from the SSP2 baseline; blue denotes welfare gains and red welfare losses. The maps share the North-South pattern but the GDP map is more saturated than the thermal map, because the permanent productivity shock shifts the steady-state capital stock and output moves by more than productivity. **Top-right:** Regional change in total factor productivity from the labour channel in 2100 (ΔTFP), plotted against the net thermal balance. The dashed line is the cross-regional OLS fit ($r = -0.98$, $R^2 = 0.96$); it shows that the thermal balance alone fixes both the sign and nearly the full magnitude of the shock. Colours distinguish the Global North (blue) from the Global South (brown). **Bottom-right:** Residuals from the fit in the top-right panel, plotted against the share of indoor (low-exposure) labour. The systematic upward trend ($r = 0.49$ across all regions, $r = 0.69$ among the heat-dominated ones) shows that the variation left unexplained by climate is governed by economic structure: outdoor-intensive economies (India, South Asia, Sub-Saharan Africa) fall below the line and lose more than their thermal balance alone would imply, because the heat penalty falls on outdoor labour, which has no cooling-adaptation channel, whereas more indoor-oriented economies (e.g. MENA) lie above it.

Energy consumption feedback and adaptation

To capture the energy-intensive adaptation response to climate-extreme variables, the model is extended to assess the endogenous adjustment of aggregate energy consumption across the residential, commercial, industrial, and agricultural sectors, with the air-conditioning capital stock evolving endogenously as part of this process. The total climate-induced shock on final energy demand is driven by regional temperature extremes and reflects the sectoral composition of energy use. These shocks quantify the percentage change in demand relative to its conditional mean associated with an additional day falling within a given temperature interval, compared with the reference interval. This framework allows us to evaluate an Adaptation Scenario (AS), in which the energy feedback mechanism responds endogenously to climate impacts according to the assumed level of adaptation capacity. The output difference relative to the Impact Scenario measures the extent to which energy-based cooling offsets the productivity losses induced by temperature extremes.

Three exploratory scenarios are evaluated, reflecting different levels of adaptation (Low, Med, High). These capture changes in energy demand arising from both autonomous adaptation by households and firms, primarily through more intensive use of adaptive appliances, and planned adaptation, in the form of increased technology adoption. In the short run, people and firms respond to temperature shocks by adjusting their use of energy-consuming appliances such as air conditioners. This immediate behavioural adjustment, referred to as the *intensive margin*, reflects changes in utilization of a fixed technology stock and therefore requires additional energy. Over longer horizons, agents interpret persistent temperature patterns as structural climatic shifts, prompting more substantial adjustments, such as households without air conditioning deciding to purchase a unit. This long-term response may be defined as planned adaptation and operates along the *extensive margin*.

The resulting adaptation scenarios are defined as follows:

Low adaptation: No additional technology is adopted relative to the baseline level. Energy responses occur exclusively along the intensive margin, with the existing technology stock held fixed at historical climate conditions. *Medium (reference) adaptation*: Long-term technology adoption is driven solely by climate change, allowing more flexible responses and higher additional energy demand than in the low-adaptation case. Expansion along the extensive margin is constrained by initial income levels, meaning that income growth does not amplify the energy-use response and AC adoption with respect to historic dose-response pattern.

High adaptation: Long-term technology adoption is driven by climate change and further amplified by higher income, reflecting an enhanced adaptive capacity to future climate risks. Both intensive and extensive-margin adjustments also vary with per-capita income, influencing the energy-intensive capital stock (AC) in addition to future climate conditions.

Results show that the energy-intensive adaptation response partially reverses the productivity and output damages of the Impact Scenario by an extent that widens with the assumed level of adaptation, but remains structurally bounded to the net thermal balance of the region and historic level of AC adoption, showing non-monotonic, and at times negative, patterns in the cold-relief, high-income Global North (Table 4).

While adaptation significantly lowers climate impacts, the global productivity in 2100 remains negative under all the three scenarios, with global means monotonically decreasing from -2.79% under Low, -2.23% under Med and -1.98% under High adaptation scenario with respect to no impact baseline, against the -3.56% impact figure.

In the Global South the energy feedback recovers a growing share of the loss. Mean productivity damage in 2100 narrows from -5.03% in the Impact Scenario to -4.05% (Low), -3.32% (Med) and -3.0% (High), offsetting, respectively, 19%, 34% and 40% of the gross loss; the same ordering holds at earlier horizons (Southern productivity loss under High adaptation of -1.54% in 2050, -2.24% in 2070). The output response inherits and amplifies this pattern through the capital channel: across the loss-making regions the permanent productivity shock shifts the steady-state capital stock, so GDP moves by more than productivity (region-level $\Delta GDP/\Delta TFP = 1.3$), and this amplification strengthens with adaptation. Mean output loss eases from -5.87% under Impact Scenario to -4.79%, -4.09% and -3.75% of projected GDP in 2100 under Low, Med, High adaptation levels (from 18% to

36% offset).

The relief is uneven across regions: the deepest end-of-century output losses still fall on India (productivity loss reduced by +37% under High adaptation, while GDP loss decreases from −11.65% to −7.51%) and Sub-Saharan Africa (TFP +28%; GDP from −8.78% to −6.38%), whereas more indoor-intensive economies recover the largest fraction of their loss, such as Brazil (TFP +60%; GDP from −7.47% to −3.10%), South Africa (TFP +57%; GDP from −3.72% to −2.39%), Latin America and the Caribbean (51%; −5.8% to −3.09%), Mexico (50%; −4.65% to −2.38%), South Asia (37%; −7.52% to −4.81%).

These outcomes show that adaptation changes the composition of the impacts, not merely their level.

The NTB / TFP relationship flattens as adaptation deepens within each adaptation scenario, from −0.0092 percentage points per net degree-day in the Impact Scenario to −0.0081, −0.0070 and −0.0065 under Low, Med and High adaptation, a roughly 29% attenuation (Table 5, panel A). These figures imply that the thermal sensitivity (net degree-days needed for a 1% productivity change) switches from ±109 net degree-days under (IS), to ±124 , ±143 , ±154, under Low, Med and High adaptation. So the climate signal is progressively reduced: it takes +12%, +31% and +41% more degree-days to move productivity by one point as adaptation deepens.

This implies that while the *NTB* effect remains the main driver, the climatic impact is cushioned.

Meanwhile, the structure of the labour force gains weight precisely under the extensive-margin adaptation scenarios (Table 5, panel B). The indoor (low-exposure) vs outdoor (high-exposure) share only marginally contributes to explaining the variance in the Impact Scenario and under intensive-margin-only Low adaptation, but its contribution roughly doubles under Med and High. Because even the extensive-margin cooling rescues indoor productivity but leaves outdoor labour exposed, the residual damage that survives adaptation concentrates on outdoor-intensive economies, and the indoor share becomes a sharper determinant of which regions are spared. Holding thermal balance fixed, the mean 2100 productivity effect of 10 more percentage points of indoor work shifts from 0.39% under (IS), to 0.29%, 0.46% and 0.43% under Low, Med and High adaptation, meaning that the weight of labour composition on total economic loss is not monotonic in adaptation levels.

A salient feature is that more adaptation does not always mean higher output. In the Global North, the averaged productivity gain is largest under Low adaptation, across all the time horizon: the Northern mean productivity change in 2100 is 1.67% under Low against 1.60% under both Med and High. The North-South wedge therefore contracts with adaptation, from 6.68 to 4.60 productivity percentage points and from 7.67 to 5.67 GDP percentage points by 2100. Three of the six Northern regions, Canada, the European Union and the non-EU Eastern European region, post higher TFP and GDP under Low than under High adaptation (Canada, for instance, 5.29% of GDP under Low versus 4.67% under High) (Table 4). These are precisely the cold-relief-dominated economies (baseline SSP2 Net Thermal Balance of -727, -346, -510, respectively), with the smallest heat exposure (ΔCDD18 of 87, 174 and 201): their advantage rests almost entirely on diminishing heating-degree-days, which remain substantially identical across scenarios, so the energy response that distinguishes Low, Med and High delivers marginally lower productivity benefit.

Two mechanisms generate this reversal. First, the protective effect of cooling energy on labour productivity saturates: the marginal mitigation of heat-driven losses diminishes with per-capita adaptation energy and plateaus beyond roughly 5-10 GJ per capita (see: Methods). Economies already energy-rich, with the United States historic averages about 7 GJ per capita and the Gulf (included in MENA) exceeds 20 GJ, against 1-2 GJ in Europe, additional cooling energy buys little further productivity, and in the cold, low-ΔCDD18 regions it buys virtually none. Second, the extensive-margin adoption that defines the Med and High scenarios carries a rising adaptation cost: the air-conditioning capital stock and energy production costs accumulate with cooling energy and their expenditure reduces consumption and capital accumulation. Because GDP is reported net of these costs, where the marginal productivity return has flattened, the additional outlay is no longer recovered and net output declines as adaptation is pushed from Low to High.

The result is an inverted incidence across the two hemispheres. In the heat-dominated South, where the cooling

channel attacks a large and binding heat penalty, the productivity benefit of additional adaptation still exceeds its cost and damages fall monotonically from Low to High. In the cold-relief North, where the benefit from diminishing cold days is proportionally higher than the impact from increasing heat ($NTB < 0$), and energy use already sits on the saturating arm of the response curve, the same escalation of energy use mostly adds cost: hence the Northern productivity mean is maximised under Low in most regions, and the most cold-relief-oriented economies are made marginally worse off by higher energy use.

This regional asymmetry is sharpest at its extremes, and the Global South is not internally homogeneous: the same saturation that depresses the Northern return re-emerges within the South wherever per-capita cooling energy is already high. The defining case is MENA. Its adaptation cooling energy is by far the largest in the group in 2050 and 2070 (Table 8), rising from about 36 GJ per capita under Low adaptation to 58 (Med) and 78 (High) by 2100, well above the Gulf's historical baseline of over 20 GJ and an order of magnitude beyond the 5-10 GJ plateau, and it carries among the heaviest air-conditioning capital outlay in the Global South (up to 13 $/person/year by 2100). Yet this energy effort buys progressively less. MENA's TFP loss still narrows monotonically ($-2.21 \rightarrow -1.84 \rightarrow -1.62\%$ in 2100), but its output, reported net of cooling costs, stops responding and even turns adverse: end-of-century ΔGDP is essentially flat between Med and High (-2.95 vs -2.96%), and at mid-century it deteriorates outright as adaptation deepens (-1.19% to -1.21% to -1.44% in 2050), so that High adaptation is never MENA's GDP-maximising scenario. The implied marginal return makes the mechanism explicit: each additional gigajoule of per-capita cooling raises MENA's net output by only 0.013 percentage points moving from Low to Med, and by -0.0005 from Med to High (essentially zero) against 0.16 and 0.06 for less energy-intensive Sub-Saharan Africa over the same steps. Because the protective response has saturated while the capital and energy bill keeps accruing, MENA's $\Delta\text{GDP}/\Delta\text{TFP}$ ratio reaches 1.83, well above the Southern regional-level norm of about 1.4, signalling that the cost channel, not the productivity channel, now governs its output.

MENA is therefore the Southern mirror of the cold-relief North: an economy pushed past its cost-effective frontier not because cooling is unhelpful in principle, but because it already operates on the flat arm of the response curve, so each further deployment mostly adds cost. The same tension appears in milder form along the rest of the high-energy tail. Latin America and the Caribbean, whose cooling energy reaches 22-34 GJ per capita under Med-High, recovers its losses by 2100 but shows the cost channel biting at intermediate horizons, where High adaptation underperforms Med (ΔGDP of -1.72 vs -1.66% in 2050 and -2.63 vs -2.42% in 2070). South Africa, at 18-26 GJ per capita under Med-High, keeps improving but carries the South's highest $\Delta\text{GDP}/\Delta\text{TFP}$ ratio (1.94), the same cost-dominance signature short of outright reversal. Even India, whose extreme-heat exposure makes its High-adaptation cooling energy the largest in the sample (about 95 GJ per capita), exhibits sharply diminishing returns at the top of the ladder: its marginal output gain per gigajoule falls from 0.034 (Low to Med) to 0.012 (Med to High), so that although adaptation still recovers roughly a third of a catastrophic loss, the final increment of energy contributes little.

The ordering of these marginal returns, i.e. declining monotonically as per-capita cooling energy rises, from Sub-Saharan Africa through India to MENA, is the descriptive counterpart of the concave, region-fixed energy effect estimated in Table 6: the pooled net return of 0.385 per log-gigajoule is an average that the energy-poor, heat-exposed economies clear comfortably and that the energy-rich Southern outliers fall well below. The cost-effective frontier of adaptation is thus not a North-South divide but a continuous function of how much cooling energy a region already deploys: it lies at low intensity in the temperate, energy-rich North, at high intensity in the hot, energy-poor South, and bends back on itself in the few hot but energy-rich Southern economies, of which MENA is the defining example, where extreme per-capita energy use places them on the same saturating, cost-dominated arm as the North despite a large and binding heat penalty.

This regional pattern proves that energy-based cooling partially offsets climate-driven labour losses but at rising welfare costs, and shows that the cost-effective frontier of adaptation is itself region-specific, lying at a lower intensity in temperate, energy-rich economies than in the hot, energy-poor South.

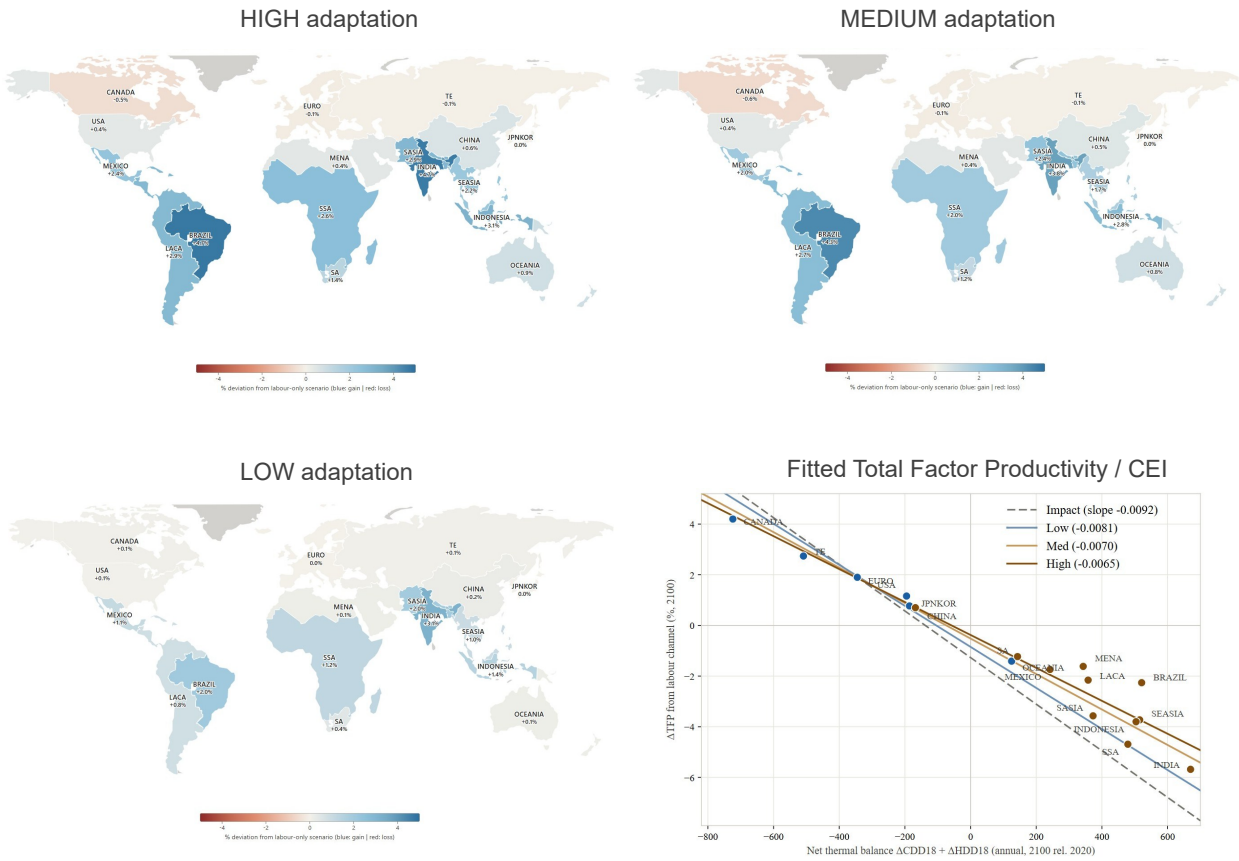


Figure 2 | Maps show the percentage change of regional GDP in 2100 with respect to the impact scenario (IS) under different adaptation levels. **Bottom-right** plots the change in total factor productivity from the labour-productivity channel in 2100 against each region's net thermal balance (NTB $= \Delta\text{CDD18} + \Delta\text{HDD18}$, the 2100 anomaly relative to 2020). The plotted markers are the seventeen WITCH regions under the High-adaptation scenario, i.e. ΔTFP measured as the percentage deviation of the High-adaptation path from the SSP2 baseline (Table 4). The four lines are the per-scenario cross-regional fits of ΔTFP on NTB (Table 5, Panel A): Impact (dashed, slope -0.0092), Low (-0.0081), Med (-0.0070) and High (-0.0065). Because the markers are the High-scenario outcomes, the solid High line is the ordinary-least-squares fit through those points (an OLS regression on the plotted data returns a slope of -0.0065 and an intercept of -0.377, reproducing the tabulated High coefficient exactly). The four lines nearly coincide in the cold-relief North (NTB < 0) and fan out in the heat-exposed South (NTB > 0): as adaptation deepens the slope attenuates monotonically by about 29%, while the correlation remains high ($|r| \geq 0.97$ in every scenario). The vertical distance between the dashed Impact line and the High line on the warm side measures how much deeper adaptation lifts the labour-productivity loss back toward zero.

Discussion

We evaluate the climate–welfare–adaptation feedback by integrating empirically estimated relationships between temperature extremes, labour productivity, and energy-intensive adaptation. In doing so, we develop a new integrated-assessment framework that bridges a long-standing gap separating two strands of the literature. Previous work on heat and labour productivity has established the size of the impact but has treated it in isolation from the energy system [14][15][3], while the cooling-energy literature has documented soaring adaptation demand and its inequality, largely on the residential margin and without closing the loop back onto productivity and output [20][22][19]. Neither strand of the literature allows damages and adaptation to co-determine one another. By endogenising the full feedback, our framework reveals how climate change reshapes the structural patterns of labour and energy demand, capturing both the damage-reducing and the redistributive nature of adaptation. Three channels operate simultaneously. First, temperature extremes depress labour productivity in ways that depend

on thermal exposure and economic structure. Second, energy demand rises endogenously through autonomous adaptation. Third, the resulting accumulation of air-conditioning capital partially insulates workers from heat, establishing a direct link between adaptation investments energy consumption and productivity.

Our results indicate that climate-induced labour impacts can lead to considerable economic losses and rising adaptation costs even in a moderate (SSP2) climate change scenario, and that these losses are deeply unequal. The negative effect on labour significantly penalises highly exposed economies in the Global South, where exposure to rising temperature is highest and adaptive capacity is more limited, while comparatively benefiting high-income regions in the Global North, which experience milder thermal stress and lower baseline vulnerability, this leading to significant distributional implications and rising inequalities within and across countries.

To isolate the specific contribution of climate change to labour productivity, we introduce a single synthetic indicator, the Net Thermal Balance (*NTB*), which aggregates the intensifying heat penalty and diminishing cold penalty. Its sign determines the direction of the productivity response: a gain where cold relief dominates ($NTB < 0$) and a loss where added heat dominates ($NTB > 0$), resulting in about $\pm 1\%$ of productivity change for every 109 net degree-days.

Projected welfare loss with respect to a baseline SSP2 scenario presents a sharp global north/south divergence that widens monotonically over the century. By 2100 the Global North experience, on average, a 1.65% of productivity gain, resulting in 1.80% of GDP, while the Global South loses roughly -5.03% and -5.87%, respectively, a difference translating in a development gap of about 7.7 GDP percentage points.

This wedge is not a static exposure gap but a divergence that the adaptation response itself widens along an energy-poverty axis. The relief that cooling delivers is governed by where a region sits on a concave, saturating response curve, and access to the arm of that curve where returns are highest is precisely what the energy-poor South lacks. The paradox is sharp: the economies with the largest unmet heat penalty (Sub-Saharan Africa, India, South Asia) are also those where each additional gigajoule of cooling would buy the most productivity, yet they enter the century with per-capita adaptation energy an order of magnitude below the level at which the protective response saturates. The binding constraint in the South is therefore not the marginal value of cooling but the access to it. Where that access exists, damage falls monotonically; where it does not, the gross heat penalty survives largely intact. Energy poverty thus converts a climatic disadvantage into a compounded economic one, and does so most severely in the outdoor-intensive economies that have no cooling channel for their most exposed workers at all, so that even fully financed cooling would leave the largest share of Southern damage untouched. The mirror image on the Northern side completes the inequity. High-income, energy-rich economies not only face a milder or negative net thermal balance, they already operate on the saturating arm of the curve, so their gains are secured cheaply and the maladaptation pattern, where it occurs, is a matter of over-spending rather than increased loss. The same energy deployment that is highly-productive in the energy-poor South may be wasted in the energy-rich North. Read through the lens of energy access, the North-South divide is therefore doubly regressive: where the South is denied the high-return adaptation it most needs, the North may afford adaptation whose return has already vanished.

The deepest end-of-century losses fall on India (-11.65% GDP), Sub-Saharan Africa (-8.78%) and Indonesia (-7.93%), while the largest gains accrue to Canada (5.18%), East-European countries including Russia (3.07%), and the EU (2.70%). China remains on the gain side (0.26%) thanks to the large cold relief of its northern latitudes, whereas Oceania (Australia and New zeland), a rich OECD region, records a net loss (-1.98%).

Despite thermal stress, the residual variation is governed by economic structure, since the heat penalty mostly falls on outdoor labour, which carries no historic adaptation channel: holding the thermal balance fixed, economies with higher outdoor/high-exposure labour share convert the same climate signal into larger productivity losses (-0.39% every 10 labour share points).

Energy-based adaptation partially reverses the climate-driven productivity and output losses, by an amount that grows with adaptation depth but stays bounded by each region's net thermal balance and its historic cooling

stock. In the heat-dominated Global South the recovery is monotonic: mean 2100 productivity loss narrows from -5.03% in the impact scenario to -4.05, -3.32 and -3.00% under Low/Med/High (a 19 to 40% offset),contracting the North-South gap from 6.68 up to 4.60 productivity points, and GDP loss from -5.87% to -4.79, -4.09 and -3.75% (18 to 36%). Relief is uneven: India and Sub-Saharan Africa remain the deepest losers, while indoor-intensive economies (Brazil, South Africa, Mexico) recover the largest share. Adaptation reshapes the composition of impacts, not just their level: the NTB-TFP slope flattens by 29%, and labour structure becomes a sharper determinant of who is spared only once extensive-margin adaptation opens. Critically, more adaptation does not always raise output: because the protective return on cooling energy saturates (5–10 GJ/capita) while AC capital and energy costs keep accruing, output is maximised under Low in most of the cold-relief North, and the same cost-dominated reversal re-emerges in hot but energy-rich Southern economies. In the cold-relief North the reversal is a productivity-channel and region-specific phenomenon: the Northern mean TFP is maximised under Low, and the three most cold-relief-dominated economies (Canada, EU, non-EU Eastern Europe) lose both TFP and GDP as adaptation deepens. It does not carry over to aggregate Northern GDP, which is dominated by the comparatively warmer, cooling-responsive USA and is highest under Med/High, a divergence between the equal-weight productivity mean and the size-weighted output aggregate that mirrors the China effect in the South.

Read together, these results describe a cost-effective frontier of adaptation that is not a North-South divide but a function of how much cooling energy a region deploys and the projected temperature increase: it lies at low intensity in the temperate, energy-rich North, at high intensity in the hot, energy-poor South, and bends back on itself in the few hot but energy-rich Southern economies.

Our results show that energy-intensive adaptation delivers real but bounded and unevenly distributed relief: it never neutralises the underlying climate signal, and its return is governed less by need than by where a region already sits on a concave, saturating response curve. The overall picture is one of twofold inequity. Across regions, the heat-exposed, energy-poor Global South bears losses several times larger than the cold-relief North, and the share recovered through adaptation is smallest precisely where the gross damage is deepest. Within the adaptation response, the same energy deployment that still pays in energy-poor economies becomes pure cost once a region crosses the saturation threshold, a form of maladaptation reached by most of the cold-relief North and by hot but energy-rich economies. Energy-intensive adaptation therefore delivers real but bounded and unevenly distributed relief. The policy reading follows directly and sharpens the case for differentiated action. Because the cost-effective frontier of cooling is region-specific rather than universal, a one-size-fits-all push for adaptation energy would be regressive on two counts: it would subsidise deployment past the point of return in the energy-rich North, while leaving unaddressed the access constraint that keeps the energy-poor South off the high-return arm of the curve entirely. Closing the North-South welfare gap therefore requires not more cooling everywhere, but energy access directed to the heat-exposed, energy-poor economies where its marginal productivity return is highest and currently unrealised, coupled with adaptation strategies for outdoor labour that no amount of space cooling can protect. Energy access for adaptation becomes a question of climate justice, since the same barrier that constrains adaptation in the South is the one that most amplifies its climate-driven losses.

Cooling energy is thus best understood as a targeted instrument with a region-specific optimal dose, a conclusion with direct implications for how adaptation policies and cooling deployment should be prioritised.

Acknowledgments

This work was supported by the European Union's *Assessing Climate Change Risk in EUrope (ACCREU)* project (Grant Agreement No. 101081358; Funding scheme: HORIZON-CL5-2022-D1-07-two-stage).

Author information

Authors and Affiliations:
Campoleoni Mansi Gabriele Alessandro[1,2,3], Colelli Francesco[2,3], Drouet Laurent[1,2,4]
[1] CMCC Foundation - Euro-Mediterranean Center on Climate Change, Via Marco Biagi 5, Lecce, 73100, Italy
[2] RFF-CMCC European Institute on Economics and the Environment, Via Bergognone 34, Milan, 20144, Italy
[3] CaFoscari University, Dorsoduro 3246, Venice, 30123, Italy
[4] CENSE - Center for Environmental and Sustainability Research & CHANGE - Global Change and Sustainability Institute, NOVA School of Science and Technology, NOVA University Lisbon, Campus de Caparica, 2829-516 Caparica, Portugal

Contributions:
The methodology and investigation were carried out by Campoleoni Mansi G. A.; Empirical estimates and model calibration were conducted by Colelli Francesco; Key contributions and supervision to the macroeconomic modelling were provided by Drouet Laurent. The authors gratefully acknowledge Enrica De Cian (Ca' Foscari University, CMCC) for her support and expertise, and Biondani Martino (Vienna Graduate School of Economics) for his contribution to the data processing.

References

[1] Van Daalen, K.R., Romanello, M., Rocklöv, J., ... et al., (2022). The 2022 Europe report of the Lancet Countdown on health and climate change: towards a climate resilient future. https://doi.org/10.1016/S2468-2667(22)00197-9

[2] International Labour Organization. (2019). Working on a warmer planet: The effect of heat stress on productivity and decent work. ILO. ISBN Web PDF: 9789221329688 https://www.ilo.org/publications/major-publications/working-warmer-planet-effect-heat-stress-productivity-and-decent-work

[3] Dunne, J., Stouffer, R. & John, J. Reductions in labour capacity from heat stress under climate warming. Nature Clim Change 3, 563–566 (2013). https://doi.org/10.1038/nclimate1827

[4] Antonelli C, Coromaldi M, Dasgupta S, Emmerling J, Shayegh S. (2020). Climate impacts on nutrition and labor supply disentangled- an analysis for rural areas of Uganda. *Environment and Development Economics* 2020; 1–26.

[5] Zivin JG, Neidell M. Temperature and the allocation of time: Implications for climate change. *Journal of Labor Economics* 2014; 32(1):1-26.

[6] Xiaodong Li, Kwan Hang Chow, Yimin Zhu, Ying Lin,. (2016). Evaluating the impacts of high-temperature outdoor working environments on construction labor productivity in China: A case study of rebar workers, Building and Environment, Volume 95, 2016, Pages 42-52, ISSN 0360-1323, https://doi.org/10.1016/j.buildenv.2015.09.005.

[7] Ballester, J., Quijal-Zamorano, M., Méndez Turrubiates, R. F., Pegenaute, F., Herrmann, F. R., Robine, J. M., ... & Achebak, H. (2023). Heat-related mortality in Europe during the summer of 2022. *Nature medicine*, 29(7), 1857-1866.

[8] Zhao, Q., Guo, Y., Ye, T., Gasparrini, A., Tong, S., Overcenco, A., ... & Li, S. (2021). Global, regional, and national burden of mortality associated with non-optimal ambient temperatures from 2000 to 2019: a three-stage modelling study. *The Lancet Planetary Health*, 5(7), e415-e425.

[9] Parsons, K. (2002). Human Thermal Environments: The Effects of Hot, Moderate, and Cold Environments on Human Health, Comfort, and Performance, Third Edition (3rd ed.). *CRC Press*. https://doi.org/10.1201/b16750

[10] Sahu S, Sett M, Kjellstrom T. Heat exposure, cardiovascular stress and work productivity in rice harvesters in India: implications for a climate change future. *Ind Health*. 2013;51(4):424-31. doi: 10.2486/indhealth.2013-0006. Epub 2013 May 20. PMID: 23685851.

[11] Schulte, P. A., Bhattacharya, A., Butler, C. R., Chun, H. K., Jacklitsch, B., Jacobs, T., … Wagner, G. R. (2016). Advancing the framework for considering the effects of climate change on worker safety and health. *Journal of Occupational and Environmental Hygiene*, 13(11), 847–865. https://doi.org/10.1080/15459624.2016.1179388

[12] Schulte, P. A., & Chun, H. (2009). Climate Change and Occupational Safety and Health: Establishing a Preliminary Framework. *Journal of Occupational and Environmental Hygiene*, 6(9), 542–554. https://doi.org/10.1080/15459620903066008

[13] Bouchama A, Knochel JP. Heat stroke. N Engl J Med. (2002) Jun 20;346(25):1978-88. doi: 10.1056/NEJMra011089. PMID: 12075060. https://www.nejm.org/doi/abs/10.1056/NEJMra011089

[14] Orlov, A., Sillmann, J., Aaheim, A. et al. Economic Losses of Heat-Induced Reductions in Outdoor Worker Productivity: a Case Study of Europe. EconDisCliCha 3, 191–211 (2019). https://doi.org/10.1007/s41885-019-00044-0

[15] Takakura, J., Fujimori, S., Hanasaki, N. et al. Dependence of economic impacts of climate change on anthropogenically directed pathways. Nat. Clim. Chang. 9, 737–741 (2019). https://doi.org/10.1038/s41558-019-0578-6

[16] Dasgupta, S., Emmerling, J. & Shayegh, S. (2023). Inequality and growth impacts of climate change—insights from South Africa. *Environmental Research Letters*, 18(12). https://doi.org/10.1088/1748-9326/ad0448

[17] De Cian, E., Pavanello, F., Randazzo, T., Mistry, M. N., & Davide, M. (2019). Households' adaptation in a warming climate. Air conditioning and thermal insulation choices. *Environmental Science & Policy*, 100, 136-157.

[18] Turek-Hankins, L. L., Coughlan de Perez, E., Scarpa, G., Ruiz-Diaz, R., Schwerdtle, P. N., Joe, E. T., ... & Mach, K. J. (2021). Climate change adaptation to extreme heat: a global systematic review of implemented action. Oxford Open Climate Change, 1(1), kgab005.

[19] International Energy Agency (IEA), (2018), The Future of Cooling, IEA, Paris https://www.iea.org/reports/the-future-of-cooling, Licence: CC BY 4.0

[20] Falchetta, G., Cian, E.D., Pavanello, F. et al. Inequalities in global residential cooling energy use to 2050. Nat Commun 15, 7874 (2024). https://doi.org/10.1038/s41467-024-52028-8

[21] Van Ruijven, B. J., De Cian, E., & Sue Wing, I. (2019). Amplification of future energy demand growth due to climate change. Nature communications, 10(1), 2762.

[22] UNCTAD (2025). Trade and finance: Reshaping the global South amid uncertainty, in *Trade and Development Report 2025*: On the brink - Trade, finance and the reshaping of the global economy, cap. IV, pp. 117–154. United Nations publication. Geneva.

[23] Riahi, K., van Vuuren, D. P., Kriegler, E., et al. (2017). The Shared Socioeconomic Pathways and their energy, land use, and greenhouse gas emissions implications: An overview. *Global Environmental Change*, 42, 153–168. https://doi.org/10.1016/j.gloenvcha.2016.05.009

[24] van Vuuren, D. P., Kriegler, E., O'Neill, B. C., et al. (2014). A new scenario framework for Climate Change Research: scenario matrix architecture. *Climatic Change*, 122(3), 373–386. https://doi.org/10.1007/s10584-013-0906-1

[25] Colelli, F.P., Emmerling, J., Marangoni, G. et al. Increased energy use for adaptation significantly impacts mitigation pathways. Nat Commun 13, 4964 (2022). https://doi.org/10.1038/s41467-022-32471-1

[26] Emmerling, J., Drouet, L., Aleluia R. L,. Bevione, M., Berger, L., and Bosetti, V., Carrara, S., De Cian, E., De Maere D'Aertrycke, G., and Longden, T., Malpede, M., Marangoni, G., Sferra, F., Tavoni, M., Witajewski-Baltvilks, J., Havlik, P. (2016). The WITCH 2016 Model - Documentation and Implementation of the Shared Socioeconomic Pathways, Fondazione Eni Enrico Mattei. 2016. Report

[27] De Cian, E.,& Wing, I., S., (2019). Global Energy Demand in a Warming Climate, *EIA: Climate Change*: Economic Impacts and Adaptation 232222, Fondazione Eni Enrico Mattei (FEEM). Handle: RePEc:ags:feemei:232222 DOI: 10.22004/ag.econ.232222

[28] Aguiar, A., Chepeliev, M., Corong, E., McDougall, R., & van der Mensbrugghe, D. (2022). The GTAP 11 Data Base. *Journal of Global Economic Analysis*, 7(2), 1–44. https://doi.org/10.21642/JGEA.070201AF

Methods

We develop a hybrid approach that explicitly disaggregates temperature-driven impacts on energy demand and labour from the aggregated damage-function in the WITCH model, enabling distinct modelling of each channel and their adaptation feedbacks. Impact-response functions on energy demand and labour productivity due to temperature extremes are empirically calibrated on a panel dataset at the country-year level and fixed effects specification including macroeconomic statistics on labour and adaptation-related energy use in productive sectors. These enable us to estimate fuel- and sector-specific responses to projected annual temperature extremes at regional scale. Following the methodology presented in Colelli et al. (2022)[25], regional temperature and the feedback on energy demand are determined endogenously by the climate emulator in WITCH and feed into further channels: the determination of AC capital stock as adaptation investments, the climate shock applied to labour productivity, weighted to the share of low- vs high-exposure sectors in the economy, and the protective effect of energy on those sectors that benefit from air conditioning. Three endogenous mechanisms are simultaneously activated: (i) First, temperature extremes reduce labour productivity differentially across countries depending on thermal exposure and the composition of the economy; (ii) Second, energy demand increases endogenously, driven by cooling and heating needs, and serves as a form of autonomous adaptation a response to permanent evolving climatic changes with respect to past climatic exposure; (iii) Third, higher energy consumption translates into greater AC capital stocks, which partially insulates workers from thermal stress, establishing a direct, endogenous link between adaptation investment and labour productivity outcomes.

Empirical estimates

We estimate the effect of CDDs and HDDs on labour productivity across sectors with different heat exposure: high-exposure (outdoor) and low-exposure (indoor) sectors. We also examine how energy use for adaptation moderates this effect.

Energy demand responses to temperature are estimated using a panel dataset of annual observations covering 134 countries over the period 1970–2019. The dataset combines three sources.

(i) First, historical per capita energy consumption, derived from International Energy Agency (IEA) statistics, is disaggregated across four sectors (residential, commercial, industrial, and agriculture) and two energy carriers

(electricity and fossil fuels).
(ii) Second, high-frequency temperature exposures from ERA5 are expressed as population-weighted Cooling Degree Days (CDD18) and Heating Degree Days (HDD18), defined as the cumulative number of degrees by which daily temperatures exceed or fall below 18 °C, respectively. Annual value measure the cumulative intensity of climate extremes over year relative to a comfort threshold (e.g. $T_{\mathrm{b}} = 18°\mathrm{C}$, hence CDD18), rather than the number of hot days. For each day d of the year, the temperature excess above (or below) the threshold is counted, and these daily excesses are summed over all days:

$$\mathrm{CDD18} \;=\; \sum_{d=1}^{N} \max\big(T_d - 18,\; 0\big), \qquad N \approx 365, \tag{1}$$

where T_d is the daily mean temperature (°C) and N is the number of days in the year. A day at $20°\mathrm{C}$ contributes 2, a day at $30°\mathrm{C}$ contributes 12, and any day at or below $18°\mathrm{C}$ contributes 0. Because each day is weighted by how far it exceeds the threshold, the annual total is not bounded by 365; as explanatory example, a Gulf country (e.g. Kuwait, Qatar, the United Arab Emirates) with a hot desert climate and an annual mean temperature of about $\bar{T} \approx 28°\mathrm{C}$, warmer than the $18°\mathrm{C}$ threshold on essentially every day of the year, may experience 3,500-4,000 CDD18 per year. These measures of Climate Extreme Indices (CEI) are used to capture the non-linear response of energy demand to temperature anomalies.
(iii) Third, economy-wide per capita GDP and per capita total capital stock are taken from the OECD dataset.
We therefore empirically estimate the semi-elasticities of final electricity and fossil fuel demand with respect to temperature extremes in each sector, distinguishing high-frequency anomalies from low-frequency trends. The resulting estimates are then used to calibrate the endogenous energy demand functions in the model.
To estimate the effect of temperature extremes on labour productivity, we use a country-year panel dataset. Labour productivity is measured as value added per worker, constructed from sectoral value added and employment statistics. The same population-weighted CDD18 and HDD18 measures described above are used, and adaptation is proxied by energy use for cooling services in productive sectors.

We estimate the following specification:

$$y_{it} = \mathrm{CDD}_{it}\,(\alpha\beta\,\text{Energy Adapt}_{it})\mathrm{HDD}_{it}\,(\gamma\lambda\,\text{Energy Adapt}_{it})X_{it}\mu_i\delta_t\phi_{r(i),t}\varepsilon_{it} \tag{2}$$

where:

- y_{it} is the logarithm of labour productivity in country i at time t,
- CDD_{it} and HDD_{it} are the number of cooling and heating degree days above the chosen threshold,
- Energy Adapt_{it} is the logarithm of per capita energy used for adaptation in productive sectors,
- X_{it} is a vector of time-varying controls, including lagged country-level capital stock and Human Capital index (HCi).
- ε_{it} is the idiosyncratic error term.

Fixed effects capture country specific heterogeneity, global shocks, and region specific trends over time.
This specification allows us to isolate the effect of thermal stress on productivity while controlling for unobserved heterogeneity across countries, global shocks, and regional trends.

Regression results Table 1 presents estimates of the relationship between temperature extremes and labour productivity under three specifications: a baseline model, a model allowing the effect of heat exposure (CDDs) to vary with adaptation energy use, and a full specification that additionally interacts cold exposure (HDDs) with

adaptation energy. Across all models, higher levels of heat and cold exposure are associated with lower productivity, with the strongest adverse effects generally observed in high exposure sectors. Introducing the interaction terms leaves the direct temperature effects largely unchanged, suggesting that the baseline estimates are robust.
The results nevertheless provide evidence that adaptation energy moderates climate related productivity losses. For heat exposure, the mitigating effect of energy use is concentrated in low exposure sectors, where greater energy consumption reduces the negative impact of high temperatures. In contrast, little evidence of heat adaptation emerges in high exposure sectors. When adaptation is also allowed to offset cold related impacts, the interaction between HDDs and energy becomes positive and significant across sector groups, indicating that energy use helps attenuate productivity losses associated with cold conditions as well. Overall, the findings suggest that productive sector energy use serves as an important adaptation channel, although its effectiveness varies substantially across sectors and is stronger in low exposure activities.

Table 1: Temperature, Energy Adaptation, and Labour Productivity

	Baseline			CDD × Energy			CDD × Energy HDD × Energy		
	Total	High Exp.	Low Exp.	Total	High Exp.	Low Exp.	Total	High Exp.	Low Exp.
Model	(1)	(2)	(3)	(4)	(5)	(6)	(7)	(8)	(9)
Variables									
Capital stock$_{t-1}$	0.3402***	0.3179***	0.3301***	0.3380***	0.3209***	0.2970***	0.3608***	0.3402***	0.3219***
	(0.0291)	(0.0371)	(0.0344)	(0.0302)	(0.0377)	(0.0366)	(0.0312)	(0.0388)	(0.0378)
HCI$_{t-1}$	0.4542**	0.4143**	0.9488***	0.4495**	0.4207**	0.8898***	0.3959**	0.3756*	0.8347***
	(0.1768)	(0.2086)	(0.1822)	(0.1756)	(0.2089)	(0.1813)	(0.1772)	(0.2104)	(0.1831)
CDDs	-0.0074	-0.0136*	-0.0054	-0.0079	-0.0129*	-0.0117*	-0.0076	-0.0126*	-0.0114*
	(0.0065)	(0.0074)	(0.0069)	(0.0065)	(0.0073)	(0.0069)	(0.0064)	(0.0073)	(0.0068)
HDDs	-0.0080**	-0.0095**	-0.0066	-0.0081**	-0.0092**	-0.0088**	-0.0073**	-0.0085*	-0.0080**
	(0.0039)	(0.0046)	(0.0041)	(0.0039)	(0.0045)	(0.0040)	(0.0037)	(0.0044)	(0.0038)
CDDs × Energy				0.0002	-0.0003	0.0028***	-0.0002	-0.0006	0.0024***
				(0.0006)	(0.0008)	(0.0007)	(0.0006)	(0.0008)	(0.0007)
HDDs × Energy							0.0009***	0.0007***	0.0009***
							(0.0002)	(0.0002)	(0.0002)
Fixed effects									
Country FE	✓	✓	✓	✓	✓	✓	✓	✓	✓
Year FE	✓	✓	✓	✓	✓	✓	✓	✓	✓
Region-year trends	✓	✓	✓	✓	✓	✓	✓	✓	✓
Fit statistics									
Observations	3,363	3,363	3,350	3,363	3,363	3,350	3,363	3,363	3,350
R^2	0.96104	0.95040	0.91202	0.96104	0.95041	0.91304	0.96143	0.95064	0.91378
Within R^2	0.08829	0.05223	0.08590	0.08836	0.05232	0.09644	0.09756	0.05670	0.10422

Heteroskedasticity robust standard errors in parentheses
Energy denotes productive-sector thermal energy use per capita (industry, commerce, and agriculture).
*Significance levels: *** p<0.01, ** p<0.05, * p<0.10*

Figure 3 illustrates how the marginal effects of CDDs and HDDs on labour productivity vary with adaptation energy use. The upper panels show that the adverse productivity effects of both heat and cold become less severe as energy use increases, consistent with the role of energy intensive adaptation measures such as cooling, heating, and climate control technologies.

For heat exposure (left panel), adaptation effects differ markedly across sectors. In low exposure sectors, the negative effect of an additional CDD declines substantially as energy use rises, indicating that adaptation can offset a large share of heat related productivity losses. By contrast, the effect remains nearly constant in high exposure sectors, suggesting more limited adaptation potential. For cold exposure (right panel), increasing energy use reduces

productivity losses in both sector groups, although the improvement is somewhat stronger in low exposure sectors.

The histogram in the lower panel reports the distribution of adaptation energy use across regions. Most observations are concentrated at relatively low energy levels, while a smaller number of countries and years exhibit substantially higher values. This distribution implies that the largest adaptation benefits shown in the upper panels are achieved only in the upper tail of the observed energy range. Overall, the figure highlights that adaptation through energy use can meaningfully reduce the productivity impacts of temperature extremes, particularly for heat exposure in low exposure sectors and for cold exposure more broadly.

Figure 3 shows that adaptation exhibits diminishing returns, with marginal benefits of cooling saturating at intermediate levels of energy use.

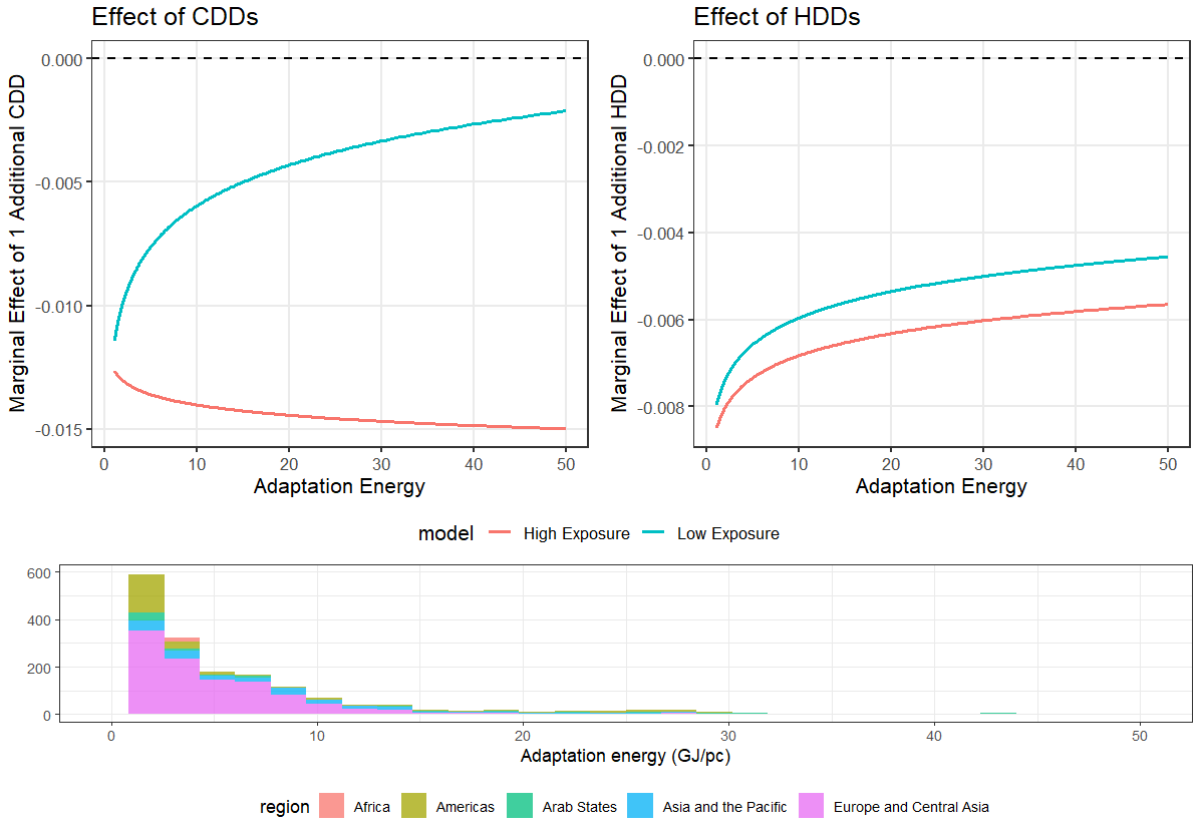


Figure 3 | Marginal change in labour productivity of high and low exposure sector, from an increase of 100 CDDs, by level of cooling energy, based on results of Table 1.

An important feature of the estimated relationship between CDDs, energy use, and low-exposure sector productivity is the clear saturation effect (Figure 3). The marginal mitigation of CDD-induced productivity losses diminishes at higher levels of per capita energy use for adaptation, with most of the effect plateauing beyond 5–10 GJ per capita. This non-linear pattern reflects diminishing returns to additional energy consumption in reducing heat-related productivity losses.

In practice, per capita adaptation energy use varies widely across countries. The United States averages around 7 GJ per capita, Europe typically ranges between 1–2 GJ, most developing countries remain below 1 GJ, while only Gulf countries exceed 20 GJ per capita. This heterogeneity implies that while additional adaptation energy could substantially reduce productivity losses in regions with low historical energy use, countries already above the 5–10 GJ threshold experience limited additional benefits.

Implementation in the WITCH model

The WITCH model [26] represents the global economy through a set of intertemporal optimisation regions linked through trade and climate externalities. The decision maker is a social planner acting on behalf of consumers and producers, who internalises both consumption and investment decisions. The production side of the economy is highly aggregated: each region produces a single commodity that can be used for consumption or investment. The final good Y is produced through a nested CES function that combines capital (K), labour (L), and energy services (ES) (Figure 4). Capital and labour are aggregated through a Cobb-Douglas production function, and this aggregate is then combined with energy services through a CES production function (Equation 3).

$$\begin{aligned} Y(t,n) = & \frac{tfp0(n)\Big(\alpha(n)\big(tfpy(t,n)\,K_{FG}(t,n)^{\beta(n)}\,l(t,n)^{1-\beta(n)}\big)^{\rho}\big(1-\alpha(n)\big)\,ES(t,n)^{\rho}\Big)^{\frac{1}{\rho}}}{\Omega(t,n)} \\ & - \sum_{f} C_f(t,n) - \sum_{ghg} C_{ghg}(t,n), \end{aligned} \tag{3}$$

where the CES parameters are $\alpha(n)$ and ρ. The parameter ρ is computed as $\rho = \frac{s-1}{s}$, where s is the elasticity of substitution, and $\beta(n)$ is the Cobb-Douglas coefficient of the capital–labour aggregate. Total factor productivity $tfpy(t,n)$ is dynamically calibrated and evolves exogenously over time. Labour l is assumed equal to population, implying no unemployment. Finally, $tfp0(n)$ is calibrated to match GDP in the base year. Energy services ES are provided by a combination of physical energy input and a stock of energy-efficiency knowledge, which allows for endogenous improvements in energy efficiency. Energy services are therefore an aggregate of the amount of energy consumed, EN, and the stock of knowledge, $RDEN$, combined within a CES function (Equation 4).

$$ES(t,n) = \phi_{ES}(n)\Big(\alpha_{ES}(n)\,RDEN(t,n)^{\rho_{ES}}\big(1-\alpha_{ES}(n)\big)\,tfpn(t,n)\,EN(t,n)^{\rho_{ES}}\Big)^{\frac{1}{\rho_{ES}}}. \tag{4}$$

Energy used in the economy is a combination of electricity and non-electric energy, the latter aggregating coal, gas and oil, both combined through a nested CES structure in which each factor is further decomposed into fuel-specific subcomponents.

$$EN(t,n) = \Big(\alpha_{EN}(n)\,EL(t,n)^{\rho_{EN}}\big(1-\alpha_{EN}(n)\big)\,NEL(t,n)^{\rho_{EN}}\Big)^{\frac{1}{\rho_{EN}}}. \tag{5}$$

Non-electric energy is obtained as a linear aggregation of its fuel components, with region-specific share parameters $\alpha_j(n)$:

$$\begin{aligned} NEL(t,n) = & \alpha_{coal}(n)\,COAL_{nel}(t,n)\alpha_{gas}(n)\,GAS_{nel}(t,n)\alpha_{oil}(n)\,OIL_{nel}(t,n) \\ & \alpha_{biom}(n)\,Biom_{nel}(t,n). \end{aligned} \tag{6}$$

Each factor is further decomposed into several sub-components, aggregated through CES, linear and Leontief production functions.

Climate impacts are introduced either as exogenous shocks or through endogenous damage functions that reduce the productivity of production factors, including physical capital, labour, energy demand, and energy supply. The standard WITCH specification aggregates climate damages across sectors and does not explicitly model sector-specific adaptation mechanisms.

The adaptation services in the standard model mitigate these aggregate impacts and are modelled through a production-based approach, as explicit endogenous choice variables. Because standard adaptation is selected by a single social planner, it cannot be assigned to specific actors or sectors; what matters is whether the action takes the form of a reactive flow of expenditures, behaving similarly to consumption, or a proactive investment that accumulates as a capital stock and depreciates over time. The effectiveness of adaptation depends on adaptive capacity, which is itself shaped by proactive investments in institutional capacity, technology, and human capital.

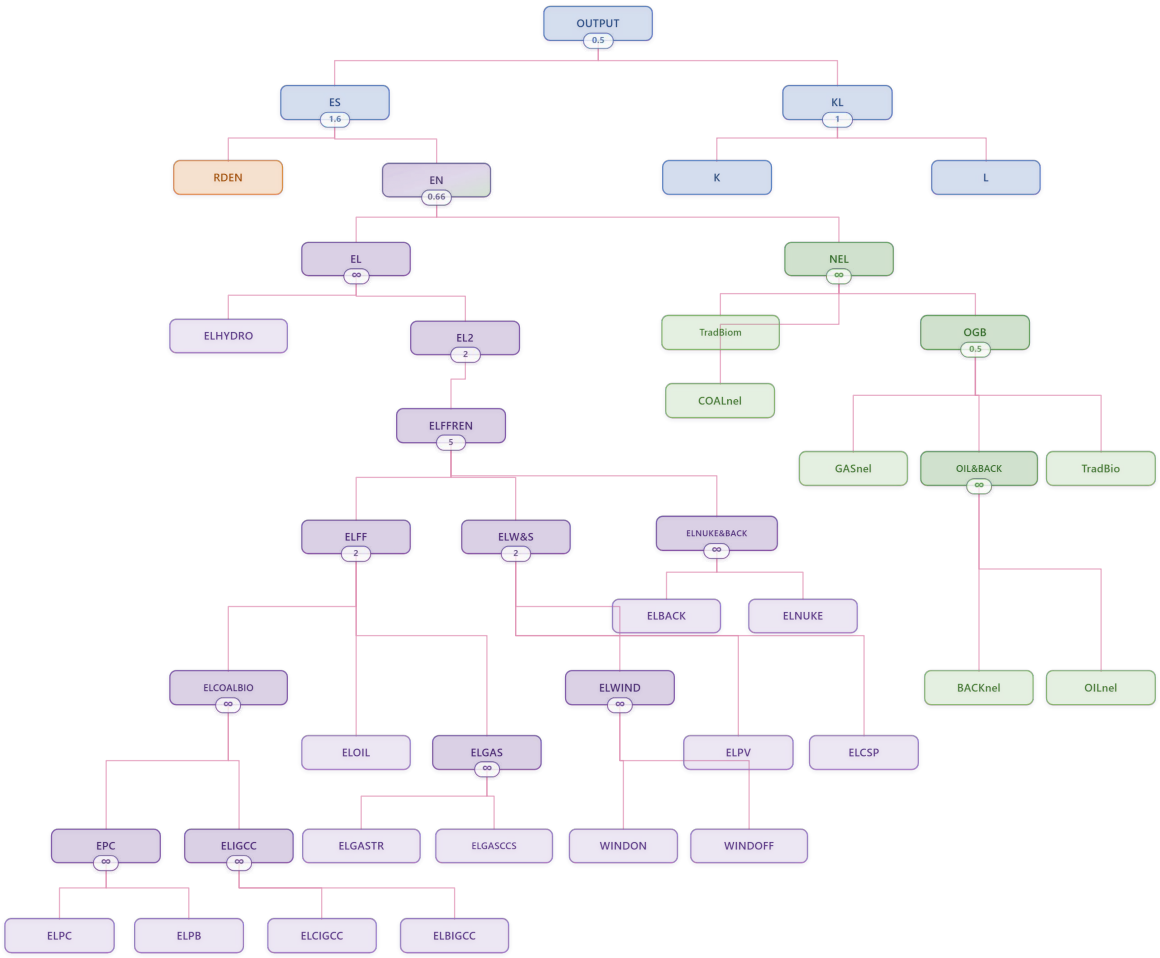


Figure 4 | CES Production Function tree of the WITCH model. The numbers under the boxes represent the production elasticities used in the energy production CES functions.

For the present study, we extend the standard model to explicitly represent the energy and labour impact channels, including the protective effect from energy increase (Figure 5). The implementation of this extended framework relies on a specific module working as a sequential, modular cascade that enables full control of the role of each component to the final outcome.

First, a statistical emulator connects the model's endogenous variable of projected global and regional near-surface average temperature to the expected regional cooling and heating degree days (CDD24s, CDD18s, HDD18s, HDD15s) used in the econometric analysis. The calibration relies on empirically estimated coefficients linking mean local temperatures with the expected number of days in which a certain temperature threshold is passed. Second, the total climate-induced shock on final energy consumption, inclusive of adaptation feedback, is implemented using empirical semi-elasticities of energy demand with respect to variations in these temperature extremes, deriving from the empirical estimates presented in the previous section. Third, the impact on labour productivity is implemented by linking endogenously-projected temperature extremes to the calibrated total factor productivity in the model, accounting for the additional energy use for adaptation. This allows us to establishing a direct, endogenous link between energy consumption, adaptation investment and labour productivity outcomes.

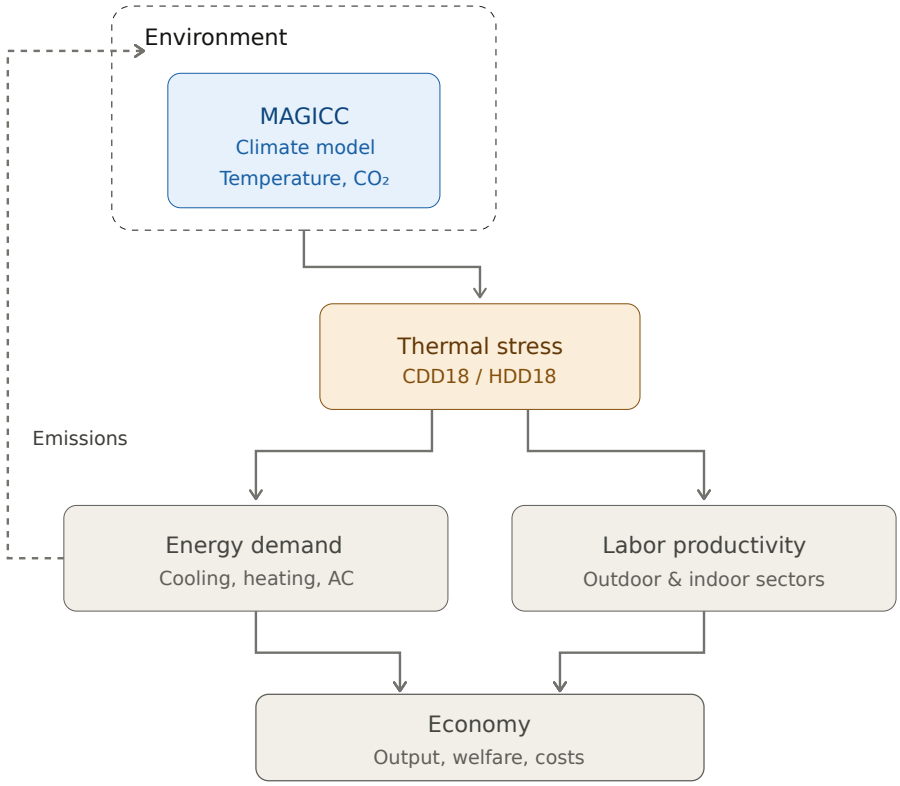


Figure 5 | The climate-energy-economy framework implemented in the standard WITCH model.

Energy demand The WITCH model is expanded to represent the impact of climate change on aggregated energy consumption across the residential, commercial, industrial and agricultural sectors, with the air conditioning capital stock evolving endogenously as part of this process.

Building on Colelli et al. (2022)[25], climate-induced changes in energy demand are implemented to reflect empirical estimates on the climate-energy relation: a warmer climate alter the energy input required to deliver a given level of output. The energy demanded-produced by the model's economy is recalibrated to match the three energy sources for which the empirical analysis provides semi-elasticities on final energy consumption, namely electricity, non-electric gas and non-electric oil, $j \in \{el,\ nelgas,\ neloil\}$, in region n at time t.

The total climate-induced shock on final energy demand, $\Phi(j,t,n)$ (`CEI_PHI` in the model), is derived from the empirically estimated semi-elasticities of energy demand with respect to the regional temperature extremes [27][25], where sector-specific coefficients have been weighted by the share of specific sector over total energy demand. These indicate the percentage by which demand shifts relative to its conditional mean level in consequence of an additional day occurring in a given temperature interval with respect to the reference temperature interval.

Let $CEI_{c^\circ}(t,n)$ denote the endogenously projected value of the climate extreme indicator c°, i.e. in Cooling Degree-Days above 24°C (CDD24) and Heating Degree-Days below 15°C (HDD15), and let $\widehat{q}_{c^\circ}(j,t,n)$ be the associated semi-elasticity (`cei_qfen` in the model). For every projection period $t \geq 2025$, the shock is computed as the proportional change in energy demand implied by moving from the climate in reference year 2020 to the

climate projected at time t:

$$\begin{aligned}\Phi(j,t,n) &= \frac{\exp\Big(\sum_{c^\circ} \widehat{q}_{c^\circ}(j,t,n)\; CEI_{c^\circ}(t,n)\Big)}{\exp\Big(\sum_{c^\circ} \widehat{q}_{c^\circ}(j,t,n)\; CEI_{c^\circ}(2020,n)\Big)} - 1 \\ &= \exp\Big(\sum_{c^\circ} \widehat{q}_{c^\circ}(j,t,n)\, \Delta CEI_{c^\circ}(t,n)\Big) - 1,\end{aligned} \tag{7}$$

where $\Delta CEI_{c^\circ}(t,n) = CEI_{c^\circ}(t,n) - CEI_{c^\circ}(2020,n)$ is the change in the climate extreme indicator relative to its 2020 value, and the sum runs over $c^\circ \in \{\mathrm{CDD24},\, \mathrm{HDD15}\}$. The exponential form reflects the semi-elasticity interpretation of $\widehat{q}_{c^\circ}(j,t,n)$: because energy demand enters the empirical specification in logarithms while the emperature extremes enter in levels, a change ΔCEI_{c° maps into a proportional energy response $\exp(\widehat{q}_{c^\circ}(j,t,n)\,\Delta CEI_{c^\circ}) - 1$. Warming simultaneously increases cooling degree-days, raising cooling-related demand, and reduces heating degree-days, lowering heating-related demand, so the net sign of Φ reflects the balance of the two channels in each region.
The semi-elasticities $\widehat{q}_{c^\circ}(j,t,n)$ are calibrated to capture the extent to which the energy-demand response adapts to a changing climate under different adaptation scenarios. Three feedback specifications are considered.
Under the high-adaptation case $\widehat{q}_{c^\circ}(j,t,n)$ follow their full estimated time path bounded to economic growth, therefore allowing for both intensive and extensive margin of energy adaptation and reflecting income amplification. Under the medium case the cooling (CDD24) semi-elasticity is held fixed at its 2020 value from 2025 onwards, reflecting that the increase of the extensive margin is bounded by initial income levels, i.e. assuming income does not amplify the energy use response. Under the low case, the 2020 cooling semi-elasticity is further rescaled by a fuel- and region-specific adaptation ratio empirically calibrated to reflects that energy responses are restricted to the intensive margin alone, i.e. existing technologies are assumed frozen at historical climate conditions. These specifications bracket the strength of adaptation operating through the energy-demand channel, while the heating (HDD15) response is left unchanged across cases.

The energy shock $\Phi(j,t,n)$ is then mapped into an absolute quantity of climate-induced adaptation energy, $ena(j,t,n)$, by scaling the calibrated baseline final energy demand of each fuel, $\widehat{Q}_{EN}(j,t,n)$,
with $j \in \{\mathrm{el}, \mathrm{nelgas}, \mathrm{neloil}\}$:

$$ena(j,t,n) = \widehat{Q}_{EN}(j,t,n)\,\Phi(j,t,n), \qquad t \geq 2025. \tag{8}$$

The mapping ensures that each fuel carries the margin it physically represents. The electricity channel reflects the cooling response through AC when an increase in CDD24 raises electricity demand. The non-electric gas and oil terms reflect predominantly heating fuels whose demand falls as HDD15s decline.
Finally, the climate feedback on energy use is closed by recalibrating final energy demand to embed the adaptation term,

$$Q_{EN}(j,t,n) = \widehat{Q}_{EN}(j,t,n)\, ena(j,t,n), \qquad t \geq 2025, \tag{9}$$

so that the model solves for an energy input that already incorporates the additional cooling demand and the foregone heating demand implied by the projected climate. The cooling-only component of the shock is further isolated by evaluating (7) with the CDD24 term only, which provides the basis for attributing the additional energy use to space cooling (air conditioning) $ena^{\mathrm{ac}}(\mathrm{el},t,n)$ and feeds the accounting of adaptation expenditure and the labour-productivity channel described below (12)(13).
The cooling energy isolated in this way represents the autonomous adaptation response as a reactive behaviour operated by households and firms, therefore determining the intensive margin of adaptation.

Adaptation costs of air-conditioning capital stock To ensure the whole adaptation feedback is described, also the proactive component of adaptation must be represented, namely the extensive margin. This is the cost of

building and operating the additional air-conditioning capital stock required to deliver the cooling service. The energy-demand feedback (8)–(9) and the air-conditioning cost channel are jointly specified to ensure consistency between the intensive and extensive margins, aligning capital stock with energy demand across the LOW, MED, and HIGH adaptation scenarios; in the LOW-adaptation case, where the technology stock is fixed at historical climate conditions, the adjustment occurs exclusively along the intensive margin.

The per-capita cost of the air-conditioning stock, $ac_stock(t,n)$, is anchored to a region-specific baseline level $AC_0(n)$ and increases with the climate-induced cooling energy per capita through an empirically calibrated (XX et al., ??), concave relationship,

$$ac_stock(t,n) = AC_0(n)\max\Big(0,\ \big[ena^{\mathrm{ac,gj}}(\mathrm{el},t,n)\big]^{0.5315}\Big), \qquad t \geq 2025, \tag{10}$$

where the exponent $0.5315 < 1$ implies that the cost of the cooling capital stock rises less than proportionally with per-capita cooling energy, consistent with diminishing marginal costs of air-conditioning provision. The additional annual expenditure relative to baseline $ac_flow(t,n)$ is aggregated to the regional level and expressed in monetary terms, and enters the economy as an energy-sector adaptation cost $COST_EN(\mathrm{ac},t,n)$ to be subtracted as the other energy and adaptation costs C_f in the output identity (3). This expenditure is borne as additional investment and crowds out resources otherwise available for consumption and capital accumulation, thereby representing air-conditioning as a proactive, stock-building form of adaptation.

Labour productivity Economic output in WITCH depends on a capital-labour aggregate and energy services through a nested production structure:

$$Y(t,n) = \Big[\Big(\alpha(n)\left(tfpy(t,n)\,K(t,n)^{\beta(n)}\,L(t,n)^{1-\beta(n)}\right)\Big)^{\rho}(1-\alpha(n))\,ES(t,n)^{\rho}\Big]^{\frac{1}{\rho}}.$$

We implemented an endogenous feedback ensuring that climate change affects the total factor productivity $tfpy$ through temperature-induced shocks, while adaptation mitigates these effects in low-exposure sectors through increased energy consumption. The evolution of productivity depends on projected changes in Cooling Degree Days above 18°C (CDD18) and Heating Degree Days below 18°C (HDD18), relative to historical level, combined with the endogenous energy used for adaptation. Formally, the climate signal enters $tfpy$ as a proportional, exposure-weighted shock relative to a baseline productivity path.

Let $tfpy_0(t,n)$ denote the baseline (climate-neutral) total factor productivity, and define the deviations of cooling and heating exposure from their historical reference levels,

$$\Delta\mathrm{CDD}(t,n) = \mathrm{CDD}(t,n) - \overline{\mathrm{CDD}}(n), \qquad \Delta\mathrm{HDD}(t,n) = \mathrm{HDD}(t,n) - \overline{\mathrm{HDD}}(n),$$

where $\overline{\mathrm{CDD}}(n)$ and $\overline{\mathrm{HDD}}(n)$ are country-specific averages computed over a fixed historical reference period. For each country we distinguish a low-exposure (indoor) and a high-exposure (outdoor) segment, with labour shares $s_L(n)s_H(n) = 1$. Actual productivity is obtained by applying the exposure-weighted shocks to the baseline path,

$$tfpy(t,n) = tfpy_0(t,n)\left[1s_L(n)\,\Pi_L(t,n)s_H(n)\,\Pi_H(t,n)\right], \qquad t \geq 2025, \tag{11}$$

where Π_L and Π_H are the proportional productivity changes induced by thermal stress in each segment.

The two segments respond to heat and cold exposure according to

$$\Pi_L(t,n) = \big(\alpha_L\beta_L \ln A(t,n)\big)\,\Delta\mathrm{CDD}(t,n)\big(\gamma_L\lambda_L \ln A(t,n)\big)\,\Delta\mathrm{HDD}(t,n), \tag{12}$$

$$\Pi_H(t,n) = \alpha_H\,\Delta\mathrm{CDD}(t,n)\big(\gamma_H\lambda_H \ln A(t,n)\big)\,\Delta\mathrm{HDD}(t,n), \tag{13}$$

where $A(t,n)$ is the total per-capita energy used for adaptation (cooling) in the productive sectors, derived from historical cooling-energy consumption level in each region and the cooling-only component of the energy demand shock $ena^{\mathrm{ac}}(\mathrm{el},t,n)$. The $\ln A(t,n)$ enters the marginal thermal responses as in the estimated specification of

Equation (2). The semi-elasticities are taken from the full empirical specification (Table 1).[1] Heat exposure carries an adaptation interaction only in the low-exposure segment ($\beta_L > 0$): cooling energy attenuates heat-driven losses where activity takes place indoors, whereas no such channel is retained for outdoor activity, consistent with the absence of a significant heat-adaptation effect in high-exposure sectors. Cold exposure carries an adaptation interaction in both segments ($\lambda_L, \lambda_H > 0$).

The equations map only the warming-consistent component of each anomaly into productivity: rising heat exposure ($\Delta\mathrm{CDD} \geq 0$) depresses productivity through the cooling-degree-day channel, while declining cold exposure ($\Delta\mathrm{HDD} \leq 0$) relieves it through the heating-degree-day channel. The specification therefore assigns productivity effects to increases in CDD and decreases in HDD, in line with the monotone warming embedded in the climate scenarios and empirical estimates.

Adaptation feedback is therefore endogenised. The adaptation energy $A(t, n)$ is the cooling-related energy demand of the productive sectors, generated by an air-conditioning capital stock that accumulates through investment in response to cooling needs: rising $\Delta\mathrm{CDD}$ raises cooling demand, the AC capital stock, and hence $A(t, n)$, which in turn dampens the heat-driven productivity loss through the positive interaction β_L. This closes an adaptation feedback in which warming simultaneously increases damages and the resources devoted to offsetting them.

To isolate the contribution of this channel, the model is solved under two regimes: a no-adaptation counterfactual (impact scenario), in which $A(t, n)$ is held at its historical level $A(t, n) = ena^{\mathrm{hist}}(n)$, so that the adaptation interaction terms remain frozen, and the adaptation scenario, in which $A(t, n)$ responds endogenously to climate impacts according to the adaptation scenario considered (LOW, MED, HIGH). The difference between the two measures the extent to which energy-based cooling offsets the productivity impacts of temperature extremes.

[1] Calibrated values (full specification): low-exposure segment $\alpha_L = -0.0114$, $\beta_L = 0.0024$, $\gamma_L = -0.0080$, $\lambda_L = 0.0009$; high-exposure segment $\alpha_H = -0.0126$, $\gamma_H = -0.0085$, $\lambda_H = 0.0007$, with no heat-adaptation interaction.
Coefficients are rescaled to the degree-day units used in the numerical model.

Extended results and data analysis

Table 2: Impact Scenario | Net Thermal Balance, Labour Productivity, Output and Labour Exposure

	Climate anomaly (2100)			ΔTFP (%)			ΔGDP (%)			Exposure (%)	
Region	ΔCDD18	ΔHDD18	NTB	2050	2070	2100	2050	2070	2100	Low	High
Global North											
Canada	87	-814	-727	2.16	3.38	4.89	2.57	4.00	5.18	89	11
East-Eur. countries	174	-684	-510	1.40	2.15	3.04	1.46	2.33	3.07	58	42
Europe	201	-547	-346	0.94	1.43	2.00	1.20	1.91	2.70	84	16
USA	302	-498	-195	0.49	0.71	0.93	0.61	0.92	1.15	90	10
Japan–Korea	208	-395	-187	0.39	0.57	0.75	0.50	0.77	1.03	73	27
Oceania	242	-116	125	-0.76	-1.26	-1.98	-0.95	-1.68	-2.76	68	32
Global South											
China	263	-432	-169	0.25	0.30	0.26	0.31	0.39	0.33	79	21
MENA	571	-227	344	-0.93	-1.57	-2.50	-1.12	-2.04	-3.36	72	28
South Africa	388	-244	144	-1.03	-1.76	-2.84	-1.28	-2.28	-3.72	71	29
Mexico	430	-187	243	-1.31	-2.18	-3.46	-1.59	-2.83	-4.65	77	23
Lat. Am. & Carib.	461	-102	360	-1.70	-2.80	-4.36	-2.06	-3.60	-5.80	74	26
SE Asia	528	-12	517	-2.12	-3.47	-5.34	-2.61	-4.46	-6.99	57	43
Brazil	579	-55	524	-2.20	-3.62	-5.68	-2.71	-4.68	-7.47	79	21
South Asia	492	-117	375	-2.18	-3.62	-5.67	-2.73	-4.72	-7.52	48	52
Indonesia	495	11	506	-2.44	-3.96	-6.02	-3.02	-5.13	-7.93	55	45
Sub-Sah. Africa	481	0	481	-2.63	-4.28	-6.54	-3.26	-5.45	-8.78	43	57
India	672	0	672	-3.55	-5.82	-8.97	-4.35	-7.40	-11.65	40	60
Regional averages											
North mean	202	-509	-307	0.81	1.22	1.65	0.88	1.37	1.80	77	23
South mean	487	-124	363	-1.89	-3.17	-5.03	-1.49	-3.07	-5.87	63	37
Global mean	387	-260	127	-1.11	-2.04	-3.56	-0.30	-1.08	-2.90	68	32

Climate columns are 2100 anomalies relative to 2020 under SSP2 baseline; NTB $= \Delta CDD18 + \Delta HDD18$ *(NTB* > 0*: heat dominates; NTB* < 0*: cold-relief dominates).* Δ*TFP and* Δ*GDP are percentage deviations of the labour-impact scenario from the SSP2 baseline,* $(x_{imp} - x_{bau})/x_{bau}$*. Exposure: share of low-exposure (indoor) and high-exposure (outdoor) labour. Components rounded independently, so aggregate values may differ by* ± 1 *from the displayed sum. Aggregate rows are ratios of scenario to baseline aggregates:* Δ*TFP is the percentage change of the (equal-weight) cross-country mean TFP, whereas* Δ*GDP is the percentage change of summed regional GDP, hence weighted by economic size.*

At mid-century the aggregate Southern GDP loss (-1.49%) is shallower than the mean TFP loss (-1.89%), an artefact of China's weight in the summed GDP rather than a genuinely milder impact. The two variables diverge when losses correlate with size: in the South, China, the largest economy, cold-relief dominated (NTB < 0) with a near-zero GDP change, pulls the summed Southern GDP toward zero, so the aggregate GDP loss looks milder than the mean-productivity loss at mid-century (2050: South ΔGDP -1.49 vs ΔTFP -1.89); this reverses by 2100 as India, a large and heavily-hit economy, comes to dominate the sum.

Table 3: Cross-regional regressions of the labour-productivity shock

	(1)	(2)	(3)	(4)
Dependent variable: ΔTFP (%, 2100)				
Net Thermal Balance	-0.0092^{***}		-0.0083^{***}	
	(0.0005)		(0.0005)	
ΔCDD18		-0.0089^{***}		-0.0085^{***}
		(0.0023)		(0.0019)
ΔHDD18		-0.0094^{***}		-0.0082^{***}
		(0.0015)		(0.0013)
Indoor (low-exposure) share			0.0388^{**}	0.0388^{**}
			(0.0131)	(0.0137)
Constant	-1.271^{***}	-1.457	-4.023^{***}	-3.937^{**}
	(0.200)	(1.261)	(0.943)	(1.352)
Observations	17	17	17	17
R^2	0.961	0.961	0.976	0.976
Adjusted R^2	0.959	0.956	0.973	0.970

*Cross-section of 17 WITCH regions at 2100. Each column is an alternative specification of the same regression, differing only in the regressors included (a blank cell means the variable is excluded). Column (1) uses the net thermal balance alone; column (2) enters cooling- and heating-degree-day anomalies separately to test whether they carry different weights; column (3) adds the indoor labour share to the net-balance model; column (4) combines the separated climate channels with the indoor share. Degree-day coefficients are per net/cooling/heating degree-day; the indoor-share coefficient is per percentage point of low-exposure labour. The constant is the model intercept, i.e. the predicted ΔTFP for a hypothetical region with zero thermal anomaly (and, in columns 3–4, zero indoor labour); it is a baseline level, not an effect of interest. Classical standard errors in parentheses. Significance: *** $p < 0.01$, ** $p < 0.05$, * $p < 0.10$.*

The cross-regional correlation between *NTB* and the change in total factor productivity (ΔTFP) in 2100 is $r = -0.98$ ($r^2 \approx 0.96$), indicating that the thermal balance alone accounts for both the sign and almost the entire magnitude of the labour-productivity shock. This translates into about one percent of change in labour productivity for every ± 109 net degree-days, depending on the sign of the net thermal balance (slope of -0.0092 percentage points of TFP per net degree-day). Estimating the two channels separately shows that cooling and heating degree-days carry essentially the same weight (-0.0089 and -0.0094 percentage points of TFP per degree-day; Table 3, column 2): the difference is within statistical error, so summing them into the equal-weighted net balance is empirically justified and leaves the fit unchanged ($R^2 = 0.96$). Net thermal balance therefore captures the climate signal with a single variable.

Combining the slope with the global-mean climate signal (387 CDD18, -260 HDD18) shows why the world does not move uniformly: the average region warms by a net 127 degree-days and the mean productivity drag across regions is about -2.4%, but this small global average masks a wide dispersion driven by the sign of the net balance, as cold, high-latitude economies gain while hot, tropical economies lose several percent.

The residual variation left unexplained by climate is governed by economic structure, namely the indoor (low-exposure) versus outdoor (high-exposure) labour split. Relative to the fitted *TFP–NTB* relationship, India, South Asia and Sub-Saharan Africa lie respectively 1.50, 0.94 and 0.83 percentage points below the line, whereas a more indoor-intensive region such as the Middle East and North Africa (which includes the Gulf countries) lies 1.94 points above it despite a very large cooling-degree-day anomaly. This pattern is systematic: the regional residuals from the net-balance fit correlate with the indoor labour share at $r = 0.49$ across all regions and $r = 0.69$ among the heat-dominated ones, and adding the share to the regression raises the explained variance from $R^2 = 0.961$ to 0.976, with a coefficient of 0.039 percentage points of TFP per additional percentage point of indoor labour (significant at the 5% level; Table 3, columns 3–4).

Table 4: Adaptation Scenario | Net Thermal Balance, Labour Productivity and Output across Adaptation Levels

	NTB (2100)			ΔTFP (%)									ΔGDP (%)								
				2050			2070			2100			2050			2070			2100		
Region	Low	Med	High	Low	Med	High	Low	Med	High	Low	Med	High	Low	Med	High	Low	Med	High	Low	Med	High
Global North																					
Canada	-720	-722	-724	2.16	2.10	2.10	3.38	3.10	3.10	4.89	4.17	4.20	2.56	2.49	2.49	4.01	3.72	3.71	5.29	4.60	4.67
East-Eur. countries	-506	-507	-509	1.40	1.36	1.36	2.15	2.04	2.02	3.03	2.78	2.74	1.47	1.44	1.44	2.34	2.30	2.28	3.16	2.99	3.02
Europe	-343	-343	-345	0.94	0.90	0.90	1.43	1.35	1.35	2.00	1.90	1.90	1.19	1.15	1.14	1.90	1.81	1.80	2.71	2.57	2.57
USA	-194	-194	-195	0.49	0.53	0.52	0.72	0.82	0.81	0.95	1.17	1.16	0.62	0.66	0.65	0.93	1.07	1.06	1.21	1.53	1.52
Japan–Korea	-185	-186	-186	0.39	0.39	0.39	0.57	0.58	0.58	0.75	0.77	0.77	0.50	0.50	0.50	0.77	0.77	0.77	1.03	1.05	1.06
Oceania	124	124	125	-0.75	-0.62	-0.62	-1.23	-0.95	-0.95	-1.91	-1.40	-1.41	-0.93	-0.78	-0.78	-1.63	-1.27	-1.26	-2.64	-1.95	-1.93
Global South																					
China	-168	-168	-168	0.27	0.32	0.33	0.37	0.48	0.50	0.44	0.66	0.70	0.34	0.40	0.41	0.48	0.63	0.65	0.56	0.86	0.92
MENA	340	341	343	-0.91	-0.87	-0.86	-1.47	-1.33	-1.27	-2.21	-1.84	-1.62	-1.19	-1.21	-1.44	-2.72	-2.39	-2.24	-3.24	-2.95	-2.96
South Africa	142	142	143	-1.01	-0.80	-0.78	-1.65	-1.08	-1.02	-2.50	-1.37	-1.23	-1.24	-1.19	-1.07	-2.14	-1.99	-1.69	-3.30	-2.61	-2.39
Mexico	240	240	242	-1.19	-1.02	-1.00	-1.84	-1.47	-1.37	-2.68	-1.99	-1.74	-1.46	-1.27	-1.23	-2.41	-1.92	-1.80	-3.64	-2.72	-2.38
Lat. Am. & Carib.	356	356	358	-1.63	-1.36	-1.33	-2.58	-1.91	-1.80	-3.75	-2.45	-2.16	-2.00	-1.66	-1.72	-3.32	-2.42	-2.63	-5.01	-3.24	-3.09
SE Asia	511	513	515	-2.01	-1.89	-1.86	-3.17	-2.88	-2.77	-4.65	-4.05	-3.73	-2.48	-2.35	-2.31	-4.07	-3.73	-3.61	-6.07	-5.40	-4.97
Brazil	518	519	521	-2.02	-1.66	-1.62	-3.04	-2.20	-2.06	-4.20	-2.63	-2.26	-2.49	-2.04	-2.04	-3.94	-2.82	-2.75	-5.58	-3.45	-3.10
South Asia	370	371	373	-1.98	-1.88	-1.84	-3.02	-2.81	-2.68	-4.27	-3.91	-3.57	-2.49	-2.37	-2.33	-3.98	-3.72	-3.56	-5.71	-5.28	-4.81
Indonesia	500	502	504	-2.25	-1.99	-1.95	-3.46	-2.94	-2.83	-5.00	-4.05	-3.80	-2.80	-2.50	-2.44	-4.51	-3.84	-3.70	-6.62	-5.39	-5.04
Sub-Sah. Africa	476	477	479	-2.54	-2.42	-2.37	-3.97	-3.67	-3.50	-5.67	-5.11	-4.69	-3.16	-3.01	-2.95	-5.08	-4.70	-4.49	-7.67	-6.94	-6.38
India	665	667	670	-3.05	-2.90	-2.80	-4.70	-4.41	-4.15	-6.80	-6.31	-5.68	-3.77	-3.60	-3.49	-6.02	-5.67	-5.39	-8.89	-8.27	-7.51
Regional averages																					
North mean	-304	-305	-306	0.81	0.81	0.81	1.23	1.21	1.20	1.67	1.60	1.60	0.88	0.88	0.88	1.38	1.40	1.40	1.84	1.92	1.92
South mean	359	360	362	-1.74	-1.58	-1.54	-2.75	-2.37	-2.24	-4.05	-3.32	-3.00	-1.36	-1.23	-1.23	-2.74	-2.36	-2.26	-4.79	-4.09	-3.75
Global mean	125	125	126	-1.00	-0.88	-0.85	-1.72	-1.44	-1.35	-2.79	-2.23	-1.98	-0.24	-0.18	-0.18	-0.89	-0.68	-0.62	-2.23	-1.76	-1.56

Climate columns are 2100 anomalies relative to 2020 reported per adaptation level; NTB = $\Delta CDD18 + \Delta HDD18$ (>0: heat dominates; <0: cold-relief dominates). Components rounded independently, so NTB may differ by ± 1 from the displayed sum.

ΔTFP and ΔGDP are percentage deviations of each adaptation scenario (L = Low, M = Med, H = High) from the SSP2 baseline at 2050/2070/2100, $(x_{ada} - x_{bau})/x_{bau}$. Aggregate rows are ratios of scenario to baseline aggregates: ΔTFP is the percentage change of the cross-country mean TFP, ΔGDP the percentage change of summed regional GDP.

Table 5: How adaptation reshapes the net-balance / labour-composition relationship: cross-regional regressions of ΔTFP by scenario

	Impact (IS)	Low adapt.	Med adapt.	High adapt.
Panel A: net balance only				
Net Thermal Balance	-0.0092^{***}	-0.0081^{***}	-0.0070^{***}	-0.0065^{***}
	(0.0005)	(0.0003)	(0.0004)	(0.0004)
Constant	-1.270^{***}	-0.848^{***}	-0.519^{**}	-0.377^{**}
	(0.200)	(0.141)	(0.181)	(0.170)
R^2	0.961	0.974	0.944	0.945
Adjusted R^2	0.958	0.972	0.941	0.941
Panel B: net balance + indoor labour share				
Net Thermal Balance	-0.0083^{***}	-0.0074^{***}	-0.0059^{***}	-0.0055^{***}
	(0.0005)	(0.0003)	(0.0003)	(0.0003)
Indoor (low-exposure) share	0.0388^{**}	0.0286^{***}	0.0461^{***}	0.0433^{***}
	(0.0131)	(0.0089)	(0.0087)	(0.0082)
Constant	-4.023^{***}	-2.877^{***}	-3.789^{***}	-3.451^{***}
	(0.943)	(0.642)	(0.627)	(0.589)
R^2	0.976	0.985	0.981	0.982
Adjusted R^2	0.973	0.983	0.979	0.979
Observations	17	17	17	17
ΔR^2 from indoor	0.015	0.011	0.037	0.037

*Dependent variable: ΔTFP (%, 2100). Cross-section of 17 WITCH regions at 2100. Each column re-estimates the same specification on the ΔTFP outcome of a different scenario; the Impact Scenario (IS) reproduces Table 3, columns (1) and (3). NTB and the indoor-share use each scenario's own values; NTB is essentially scenario-invariant, so cross-column differences reflect the changing ΔTFP response rather than changing regressors. Classical standard errors in parentheses. Significance: *** $p < 0.01$, ** $p < 0.05$, * $p < 0.10$.*

Re-estimating the NTB / TFP relationship within each adaptation scenario (Table 5), the slope of ΔTFP on *NTB* flattens monotonically as adaptation deepens, from -0.0092 percentage points per net degree-day in the Impact Scenario to -0.0081, -0.0070 and -0.0065 under Low, Med and High adaptation, a roughly 29% attenuation, with the correlation staying high ($|r| \geq 0.97$): while the *NTB* effect remains the main driver of impact, the climatic signal is cushioned. Meanwhile, the structure of the labour force gains weight precisely under the extensive-margin adaptation scenarios: adding the indoor (low-exposure) share raises the explained variance only marginally in the Impact Scenario (R^2 from 0.961 to 0.976; coefficient 0.039) and under intensive-margin-only Low adaptation ($0.974 \rightarrow 0.985$; 0.029), but its contribution roughly doubles under Med and High (0.944 to 0.981 and 0.945 to 0.982; coefficients 0.046 and 0.043, $p < 0.001$).

Under Low adaptation, labour composition matters less than in the Impact case. Low adaptation is intensive-margin only: it can raise cooling intensity where AC stock already exists, applying a homogeneous buffer bounded to the historically installed capacity. That stock is concentrated in the Global North, a region that combines a negative net thermal balance with a high indoor share (Table 2). There, climate change works mainly through the easing of cold-related productivity losses rather than through rising extreme heat, so the marginal value of additional cooling is low or even negative: running AC harder buys little, because the shock is dominated by the removal of cold penalties, not by a surge in heat penalties. Low adaptation therefore spends its effort exactly where heat, and hence the indoor/outdoor distinction, is not the binding constraint, while the heat-exposed economies of the South, where cooling would discriminate sharply between shielded indoor and unshielded outdoor work, receive no proportional expansion of coverage. Because the buffer is homogeneous and capacity-bound rather than targeted at heat, it never activates the labour split as a protective margin: it leaves composition a passive background condition and, by uniformly cushioning the already-protected North, slightly erodes its discriminating power.

By contrast, in the extensive-margin adaptation scenarios (Med and High), there is a deliberate increase in AC coverage beyond the intensive margin, yet this expansion is confined to indoor labour. This means that, on the one hand, the indoor sector becomes progressively more resilient to climate change through accumulating new cooling capital; on the other hand, the outdoor sector remains equally exposed and impacted, receiving no equivalent technological buffer. Consequently, as indoor productivity is increasingly shielded, the burden of the residual climate damage shifts disproportionately onto the outdoor workforce. The share of outdoor labour therefore progressively acquires greater weight in determining the final economic impact, pushing the economic structure from a passive background condition into the central bottleneck of adaptation effectiveness. This is exactly why the coefficient for the indoor share increases under Med and High relative to the Impact case, while it actually falls under Low: the former scenarios redraw the geography of impacts, concentrating the surviving damage on the unshielded outdoor workers, whereas the latter merely applies a flat, capacity-constrained buffer that erases the discriminative power of the labour split.

Table 6: Net protective effect of adaptation energy on output: scenario×region×horizon panel of ΔGDP

	(1)	(2)	(3)
Dependent variable: ΔGDP (%); panel of 17 regions × 3 scenarios × 3 horizons			
Net Thermal Balance	-0.0087^{***}	-0.0087^{***}	
	(0.0002)	(0.0003)	
Indoor (low-exp.) share	0.0323^{***}	absorbed	absorbed
	(0.0031)		
ln(adaptation cooling energy)	0.206^{***}	0.303^{***}	0.385^{***}
	(0.050)	(0.049)	(0.037)
			[0.106]
Scenario FE	yes	–	–
Time FE	yes	yes	–
Region FE	no	yes	–
Region × Horizon FE	no	no	yes
Observations	153	153	153
R^2	0.978	0.985	0.994

Panel of 17 WITCH regions × {Low, Med, High} × {2050, 2070, 2100}. NTB and adaptation cooling energy (per-capita AC energy, GJ/person, in logs) vary by scenario, region and horizon; the indoor share is region-fixed and is absorbed once region effects are included. ΔGDP is net of air-conditioning costs, so the energy coefficient is the net *output effect of adaptation. In column (3) climate and structure are held fixed within each region×horizon cell, so the energy coefficient is identified purely from across-scenario variation; classical standard error in parentheses, region-clustered in brackets. Significance: *** $p < 0.01$.*

To isolate the net contribution of energy-based cooling to output, Table 6 pools the three adaptation scenarios into a single panel of 17 WITCH regions $\times\{Low, Med, High\} \times \{2050, 2070, 2100\}$ (153 observations) and regresses ΔGDP on the net thermal balance (*NTB*), the indoor (low-exposure) labour share, and per-capita adaptation cooling energy entered in logs. Two features are explained. First, the dependent variable is output measured *net* of energy costs (capital outlay plus energy expenditure), so the coefficient on cooling energy already nets out what adaptation costs to deploy. Second, the log specification lets each additional gigajoule deliver a diminishing marginal effect, embedding the saturation of the protective response documented above.

The estimated effect of cooling energy is positive and highly significant throughout, and strengthens as the specification tightens the identification (0.206 with scenario and time fixed effects, 0.303 once region effects are added, 0.385 under region × horizon effects, all p<0.01; region-clustered standard error 0.106 in the most demanding column). The two structural regressors behave as expected: *NTB* carries a negative coefficient (-0.0087), confirming that the climatic penalty remains the dominant driver of output, while the indoor share enters positively (0.0323)

but is mechanically absorbed once region fixed effects are introduced, since it is region-invariant. The decisive column is (3): with region $\times$ $\times$horizon effects, climate, labour structure and the development path are all held fixed within each cell, so the energy coefficient is identified purely from the $Low \rightarrow Med \rightarrow High$ variation in deployed cooling. The fact that it stays positive and significant establishes that, on average across regions, additional adaptation energy raises net output even after its own cost is subtracted, providing the panel counterpart to the *partial offset* obtained in the scenario results. Because the energy term is logged, this average return is concave: the model attributes the largest net gains to energy-poor, heat-exposed economies and progressively smaller ones as per-capita cooling rises, which is precisely why the average net effect is positive while the cold-relief, energy-rich North can still be made marginally worse off by further adaptation.

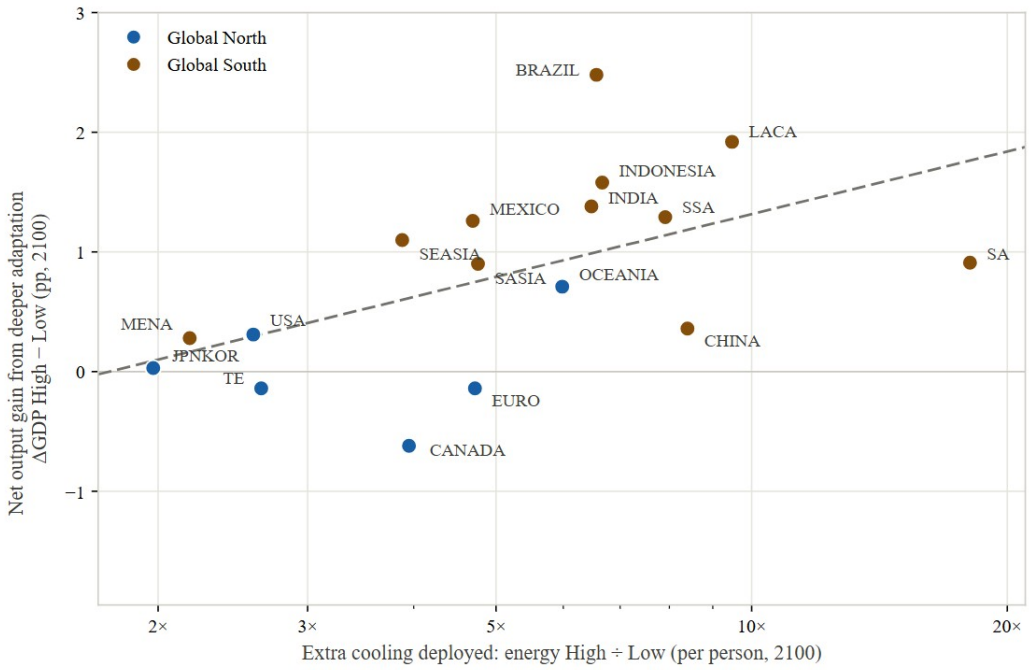


Figure 6 | summarises the net output return to deploying more cooling, keeping the same Low-versus-High contrast. For each region the vertical axis is the net output gain obtained when moving from Low to High adaptation in 2100, computed as $\Delta\mathrm{GDP}(\mathrm{High}) - \Delta\mathrm{GDP}(\mathrm{Low})$ from the ΔGDP columns of Table 4 (ΔGDP is the deviation from the SSP2 baseline. The horizontal axis shows how much additional cooling is actually deployed in that move, expressed as the ratio of per-capita air-conditioning energy (GJ/person) under High to that under Low in 2100 (Table 8) and shown on a logarithmic scale; plotting the ratio on a log axis is equivalent to differencing log energy between the two scenarios, which is the dose that pairs with the log-energy specification of the panel regression. The dashed line is an OLS fit through the seventeen points (slope $\approx +0.76$ per log-unit of extra cooling, $r = 0.53$). This raw 2100 contrast is sharper than the cost-net panel estimate of $+0.385$ obtained from the full region $\times$ scenario $\times$ horizon regression (Table 6, column 3), because 2100 is the horizon with the largest cooling expansion; the two numbers describe different objects (a single end-of-century contrast versus the average within effect across all horizons). The figure shows that the Global South lies above the line (each extra unit of cooling buys real output) whereas the cold-relief North gains little and can turn negative (Canada deploys several times more cooling yet loses net output), with visible saturation in already-cooled economies such as the Gulf-heavy Middle East and North Africa and in very high-coverage cases such as South Africa.

Table 7: Adaptation Scenario | Final energy: climate-driven change and percentage deviation

	ΔENA (TWh)									Shock EN (%)								
	2050			2070			2100			2050			2070			2100		
Region	Low	Med	High	Low	Med	High	Low	Med	High	Low	Med	High	Low	Med	High	Low	Med	High
Global North																		
Canada	-33.6	-29.5	-28.8	-51.3	-19.7	-18.5	-64.1	25.1	22.1	-1.4	-1.2	-1.2	-2.6	-1.0	-0.9	-3.9	2.0	1.9
East-Eur. countries	-48.1	86.8	106.8	-110.6	177.8	240.7	-187.9	334.8	506.0	-0.6	0.6	0.8	-1.0	1.3	1.8	-1.6	2.5	3.9
Europe	-95.4	227.3	255.3	-152.2	399.3	436.4	-199.2	586.1	653.6	-0.9	1.5	1.7	-1.3	2.9	3.1	-1.8	5.0	5.6
USA	-109.4	523.7	495.7	-164.5	955.2	881.0	-209.4	1428.0	1262.1	-2.2	1.9	1.7	-1.2	6.6	6.1	-1.7	11.3	10.0
Japan–Korea	-8.1	87.5	94.7	-10.1	121.3	122.4	-8.8	138.4	132.0	-0.2	2.0	2.2	-0.4	3.7	3.7	-0.5	6.3	6.0
Oceania	-8.4	32.7	35.0	-14.2	62.2	65.3	-14.3	97.8	97.8	-0.6	2.2	2.4	-0.9	4.0	4.2	-1.0	6.4	6.4
Global South																		
China	35.0	1115.9	1417.7	-14.0	1636.4	2254.4	-97.1	1883.0	2858.5	0.2	3.0	3.8	0.2	5.1	6.9	1.4	9.7	13.8
MENA	171.8	1154.0	1322.1	713.2	3271.7	4230.6	1552.6	6744.9	10782.0	-1.2	5.1	6.1	3.5	16.6	21.5	8.1	32.6	51.6
South Africa	-1.0	39.9	47.3	-5.7	129.8	168.7	-12.0	279.2	403.9	-2.4	0.6	1.1	-0.3	7.2	9.3	1.1	14.8	20.6
Mexico	-7.3	112.6	135.7	6.3	255.9	348.0	66.5	462.8	732.9	-0.4	4.3	5.2	0.1	7.9	10.8	1.8	13.4	21.3
Lat. Am. & Carib.	22.6	348.5	413.9	71.5	907.1	1207.1	158.9	1938.8	3014.4	-0.1	5.5	6.6	0.9	11.8	15.8	1.7	21.5	33.5
SE Asia	267.7	741.9	896.0	525.8	1543.3	2136.9	902.7	2891.4	4994.6	4.2	11.8	14.3	7.7	22.8	31.6	13.2	42.4	73.2
Brazil	62.1	320.7	370.3	152.6	820.0	1038.6	300.1	1709.7	2484.3	1.3	6.3	7.2	2.1	11.6	14.7	3.6	20.6	30.0
South Asia	106.5	285.9	373.2	373.6	1018.4	1625.1	1159.0	3250.2	7026.1	2.4	6.4	8.4	5.1	13.9	22.2	9.4	26.6	57.6
Indonesia	99.4	414.4	510.0	199.5	915.6	1222.4	319.5	1687.4	2583.8	3.0	12.7	15.7	5.5	25.5	34.0	8.9	47.1	72.2
Sub-Sah. Africa	105.6	364.3	533.0	415.6	1468.4	2742.6	1536.1	5616.1	14190.7	0.9	3.2	4.7	2.0	7.2	13.5	4.1	14.5	36.3
India	1279.8	2585.9	3966.2	2940.9	6263.8	12299.5	5523.9	12723.4	36738.5	7.1	14.4	22.1	13.5	28.7	56.5	23.2	53.6	155.0
Regional averages																		
North mean	-50.5	154.7	159.8	-83.8	282.7	287.9	-113.9	435.0	445.6	-1.0	1.2	1.3	-1.2	2.9	3.0	-1.7	5.6	5.6
South mean	194.7	680.4	907.8	489.0	1657.3	2661.3	1037.3	3562.4	7800.9	1.4	6.7	8.7	3.7	14.4	21.5	7.0	27.0	51.4

Per-region results of each adaptation scenario (Low/Med/High) at 2050/2070/2100. ΔENA: climate-induced net energy change (cooling EN + heatig EN) in total final energy consumption (TWh) with respect to baseline SSP2. Shock EN: percentage deviation of total final energy consumption (TWh) in adaptation scenarios from baseline, $(x_{(AS)} - x_{BS})/x_{BS}$, by year. Regional means are unweighted averages across regions.

Table 8: Adaptation Scenario | Air-conditioning energy and capital across adaptation levels

	AC Gj (GJ/person)									AC stock ($/person/yr)								
	2050			2070			2100			2050			2070			2100		
Region	Low	Med	High	Low	Med	High	Low	Med	High	Low	Med	High	Low	Med	High	Low	Med	High
Global North																		
Canada	3.08	3.89	3.94	3.10	6.64	6.72	3.14	12.72	12.40	6.00	6.90	6.93	6.00	7.97	7.99	6.00	9.34	9.28
East-Eur. countries	3.56	4.61	4.76	3.62	5.91	6.40	3.75	8.47	9.92	4.43	5.48	5.56	4.43	6.03	6.19	4.43	6.77	7.12
Europe	1.54	3.49	3.63	1.58	5.15	5.31	1.62	7.34	7.65	4.43	5.87	5.92	4.43	6.42	6.47	4.43	6.98	7.05
USA	8.10	14.07	13.71	8.37	18.75	17.92	8.64	24.11	22.37	4.48	7.15	7.07	4.48	8.07	7.92	4.48	8.90	8.65
Japan–Korea	4.47	6.33	6.48	4.52	7.60	7.63	4.58	9.23	9.04	3.91	5.34	5.39	3.91	5.77	5.78	3.91	6.23	6.18
Oceania	0.99	3.08	3.22	1.07	4.83	5.00	1.17	7.00	7.00	3.91	5.43	5.48	3.91	5.99	6.04	3.91	6.53	6.53
Global South																		
China	0.84	3.59	4.37	1.20	6.28	8.14	1.69	10.17	14.20	2.55	4.41	4.64	2.55	5.12	5.52	2.55	5.91	6.59
MENA	26.28	29.85	30.74	29.82	39.69	44.31	35.70	58.01	77.79	4.35	6.90	7.10	4.35	8.67	9.30	4.35	10.86	12.66
South Africa	0.73	2.59	2.96	0.95	7.46	9.46	1.43	18.43	25.85	4.06	5.48	5.63	4.06	6.83	7.24	4.06	8.68	9.62
Mexico	1.88	3.79	4.29	2.78	7.26	9.33	4.19	13.02	19.67	3.99	5.67	5.83	3.99	6.61	7.05	3.99	7.72	8.71
Lat. Am. & Carib.	1.86	4.90	5.55	2.43	10.39	13.32	3.55	22.22	33.66	3.99	5.92	6.10	3.99	7.19	7.71	3.99	9.00	10.32
SE Asia	6.39	9.98	11.16	8.41	16.18	20.74	12.05	28.88	46.72	3.91	6.43	6.70	3.91	7.64	8.34	3.91	9.40	11.24
Brazil	2.86	7.02	7.82	4.45	15.80	19.51	7.89	36.23	51.80	3.99	6.39	6.58	3.99	8.05	8.59	3.99	10.55	11.99
South Asia	0.96	1.70	2.14	2.34	4.78	7.46	6.45	14.47	30.71	3.91	5.11	5.29	3.91	6.13	6.76	3.91	8.00	10.05
Indonesia	2.18	5.78	6.87	3.36	11.67	15.23	5.19	22.97	34.61	3.91	6.20	6.47	3.91	7.43	8.01	3.91	9.07	10.39
Sub-Sah. Africa	0.51	0.95	1.23	0.87	2.25	3.92	2.03	6.55	16.06	3.91	4.69	4.86	3.91	5.33	5.89	3.91	6.56	8.24
India	3.26	6.12	9.16	7.04	14.46	27.98	14.63	33.10	94.74	3.91	6.43	7.08	3.91	7.99	9.74	3.91	10.29	15.12
Regional averages																		
North mean	3.62	5.91	5.96	3.71	8.15	8.16	3.82	11.48	11.40	4.53	6.03	6.06	4.53	6.71	6.73	4.53	7.46	7.47
South mean	4.34	6.93	7.85	5.79	12.38	16.31	8.62	24.00	40.53	3.86	5.78	6.02	3.86	7.00	7.65	3.86	8.73	10.45

Per-region results of each adaptation scenario (Low/Med/High) at 2050/2070/2100. AC Gj: total per-capita energy consumption for air-conditioning cooling (GJ/person). AC stock: capital investment for air-conditioning ($/person/year). Regional means are unweighted averages across regions.

All data, extended material and appendices are available on GitHub: